

Entanglement Wedge Reconstruction and Correlation Measures in Mixed States, Modular Flows versus Quantum Recovery Channels

Mahdis Ghodrati^{a,b,c}

^a*Department of Physics, Sharif University of Technology, Tehran 1458889694, Iran*

^b*Shing-Tung Yau Center of Southeast University, Nanjing 210096, China*

^c*Center for Gravitation and Cosmology, Yangzhou University, Yangzhou 225009, China*

E-mail: mahdisg@yzu.edu.cn

ABSTRACT: In this work we study the nature of correlations among mixed states in the setup of two symmetric strips. We use various tools to determine how the bulk geometry could be reconstructed from the boundary mixed information. These tools would be modular Hamiltonian and modular flow, OPE blocks, quantum recovery channels such as Petz map, Uhlmann holonomy and Wilson lines. We comment on the similarities and connections between these approaches in our setup of mixed states. Specially, we use parameters such as dissipation which is being modeled by the mass of graviton, and also the same sign charges of the two strips to find connections between these different approaches. Also, using Uhlmann fidelity as the correlation measure, we look into the various types of correlations such as discord. We then use simple results of modular Hamiltonian for fermions to get information about the relations between modular flow and entanglement and complexity of purification (EoP/CoP) and also modular flows of confining geometries. Finally, we study the dynamics of correlations using various information speeds and then model of void formation in CFTs and again we comment on their relationships with EoP and CoP.

Contents

1	Introduction	1
2	The Setup	3
3	Entanglement Wedge Cross Section and Modular Flow	7
3.1	Quantum recovery channels versus modular flows in mixed states	12
3.2	Complexity, Berry phase and modular Hamiltonian	22
3.3	Modular Hamiltonian, connected vs. disconnected regions	32
3.4	The effects of dissipation and charge on CC flow and kink transform	34
3.5	Entanglement wedge cross section from OPE blocks	37
3.6	Uhlmann holonomy for mixed states	39
4	Correlation Measures for Mixed States and Quantum Discord	42
5	Modular Hamiltonian in QCD	46
6	Dynamics of Correlation Exchanges	49
6.1	Information speed in mixed setup	50
6.2	Void formation in mixed states	54
7	Discussion	58

1 Introduction

In the setup of holography, the conjecture is that out of information and entanglement in the boundary field theory, the one dimension higher bulk geometry could be reconstructed. Various models of bulk reconstruction has been discussed in the literature which have been dubbed HKLL [1], DHW [2], ADH [3], and FL [4]. There is another approach which uses extremal area variations [5]. Various models of tensor networks and also quantum error corrections have been employed for the bulk reconstruction.

Most of these methods of the bulk reconstruction, used the subregion/subregion duality and quantum error correction and they were used in a fixed background.

Recently, new works on the connections between geometry in the bulk and information on the boundary CFT, in the setup of modular Berry connection and Berry curvature of modular Hamiltonians [6], see also [7, 8], have been presented. In lights of these developments, our motivation in this work is to clarify several points in

our previous work [9] and determine how in mixed quantum systems, modular flow or quantum recovery channels and other approaches of bulk reconstructions, would work and what would be the connections between these approaches.

To do this, we implement these approaches in several backgrounds with charge or in massive gravity backgrounds where the graviton has a finite mass that simulates dissipation in the model. By changing the charge of the strips q or the mass of graviton m , in different approaches, we track the change in the bulk reconstruction formulations to seek their connections. Also, the specific effects of these parameters on bulk reconstruction methods and the change in various correlation measures, in particular the entanglement and complexity of purification (EoP/CoP) would be discussed.

Here, we actually consider a symmetric setup where the two strips have the same width l , with a distance D between them. One of the motivations in this work is to understand how the modular flow, modular zero modes, soft modes or edge modes and modular Hamiltonian would change when the two subregions move from far distances (when $I = 0$ or EoP = 0 to a closer distance to each other ($I \neq 0$ and EoP $\neq 0$), where the system undergo a phase transition from two pure sub-spaces to one mixed system. This would actually be done by tracking the extremal surfaces at each stage of the evolution.

We are also specially interested to check the connections between modular chaos and quantum recovery channels, since both of these proposals could point out how the bulk curvature and bulk spacetimes could emerge from the dual boundary CFT data. Note that in general quantum information are being processed in quantum channels where by passing time, more errors would be accumulated. On the other hand, under modular evolution, the modular Hamiltonian become more and more non-local and get larger commutators with all other operators of the system. Therefore, we expect to observe more connections between these two formulations of bulk reconstruction. Another hint came from the value of conical 2π at the x -axis in the connected entanglement wedge part which is actually related to the 2π constant of CoP in $2d$ that we found in [9].

In addition, in [10], the connections between universal recovery channels and modular Hamiltonian have been noticed as they showed that by perturbing a bulk state in a direction of a bulk operator which is within a boundary subregion the modular Hamiltonian of the boundary would correspondingly respond which is related to the non-commutative version of Bayes rule which can be used to generate and reconstruct the lost information similar to a quantum error correction system.

Note also that, the connections between thermal quantum chaos and quantum recovery channels have already been discussed in quantum information literature, so we expect such connections also work for modular chaos and quantum error corrections which then could give us further information about the mechanisms of bulk emergence. So the connections between various universal recovery channel such as

twirled Petz map or normal Petz map and modular Berry flow and also symplectic form would be discussed.

As a matter of fact, most of the discussions in bulk reconstructions have been done for pure states. Here we are specially interested in a mixed setup. The connections between modular Berry connection and entanglement wedge for pure systems has been discussed in [6, 7, 11] and for the case of mixed states in [12], where it has been proposed that the Berry phase along the “Uhlmann parallel paths” would be the integral of a connection which its curvature would be the symplectic form of entanglement wedge (E_W). So Berry phase and the symplectic form of E_W , has been related in that work. Then, in [13], the reconstruction of entanglement wedge using Petz map has been discussed. Using these works, one specifically could draw connections between Petz map and Berry and Uhlmann phase, modular connections and also the symplectic form of E_W . Also, the connections between quantum error correcting properties of holography and modular flow, modular connection, and symplectic form of entanglement wedges could be noticed.

Also, note that most of the discussions of holographic bulk reconstructions using error corrections have been done in two dimensional JT gravity background, while our setup of two intervals in the AdS₃ background, would be richer than those discussed in [13, 14]. Specially the Petz map in the real $3d$ case should be considered.

One interesting phenomenon would be the phase transitions between zero mutual information (MI) between the strips when they are far apart and a jump in MI when they get closer than a critical distance D_c . As Berry curvature of modular Hamiltonians could sews together the orthonormal coordinate systems along the HRRT surfaces and lead to the bulk reconstruction, [6], we would like to examine this proposal for the case of two disconnected versus connected subsystems and then investigate the properties of the modular Hamiltonian, modular flows and Berry connection for each case and also during the phase transition.

We first start with explaining our setup and then step by step discuss various approaches and sketch the connections between them.

2 The Setup

Our setup consist of two subregions A and B which are infinite strips with the width of l separated by the distance D on the same side of the boundary as

$$\begin{aligned} A &:= \{l + D/2 > x_1 > D/2, -\infty < x_i < \infty, i = 2, 3, \dots, d - 1\}, \\ B &:= \{-l - D/2 < x_1 < -D/2, -\infty < x_i < \infty, i = 2, 3, \dots, d - 1\}, \end{aligned} \quad (2.1)$$

which is shown in figure 1.

The critical distance D_c for each dimension could actually be found by setting the mutual information $I(D, l) = 0$ in each case as we did in our previous work. The

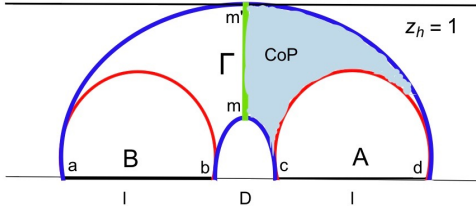


Figure 1. Two strips of A and B with length l and with the distance D between them is shown. The two turning points would correspond to region ad and bc which are m and m' , and Γ is the minimal cross section of the “connected” entanglement wedge.

mutual information of AB would be

$$I(D, l) = S_A + S_B - S_{AB} = 2S(l) - S(D) - S(2l + D). \quad (2.2)$$

The background was chosen to be the Schwarzschild AdS black brane in the form

$$ds^2 = \frac{1}{z^2} \left[-f(z)dt^2 + \frac{dz^2}{f(z)} + d\vec{x}_{d-1}^2 \right], \quad f(z) := 1 - z^d/z_h^d. \quad (2.3)$$

The entanglement of purification (EoP) between these two states could be computed using the area of the surface Γ shown in green and the complexity of purification (CoP) of the volume of blue region as we showed in [9].

In that work, we also studied the effects of charge q and mass of graviton m on EoP and CoP by considering such background as the metric of charged-massive BTZ black hole in the following form [15]

$$ds^2 = \frac{1}{z^2} \left[-f(z)dt^2 + \frac{dz^2}{f(z)} + dx^2 \right] \quad \text{with} \quad f(z) = -\Lambda - m_0 z^2 - 2q^2 z^2 \ln\left(\frac{1}{z\ell}\right) + m^2 c c_1 z, \quad (2.4)$$

which is a solution to Einstein equations for the three dimensional Einstein-massive gravity with the action [15]

$$\mathcal{I} = -\frac{1}{16\pi} \int d^3x \sqrt{-g} \left[\mathcal{R} - 2\Lambda + L(\mathcal{F}) + m^2 \sum_i^4 c_i \mathcal{U}_i(g, h) \right], \quad (2.5)$$

where \mathcal{R} is again the scalar curvature, $L(\mathcal{F})$ is an arbitrary Lagrangian of electrodynamics and Λ is the cosmological constant.

In 2.4, m_0 is just an integration constant which is related to the total mass of black hole where we set $m_0 = 1$. In addition, in the following study, we set $c = c_1 = 1$, without any loss of generality.

So our solution is a “massive-charged BTZ black hole” in a “massive gravity theory” where the graviton has the finite mass m . Here we very are interested in studying the effects of the parameters m and q on various bulk reconstruction formulations such as quantum error corrections, modular flow, CC flow OPE block,

etc. Also, the effects of dimension of the boundary d on the bulk reconstruction procedure could be considered.

Note that in the action, m is the mass of graviton in the theory. In the holographic framework, the massive terms in the gravitational action break the diffeomorphism symmetry in the bulk, which then would correspond to momentum dissipations in the dual boundary field theory as shown in [16].

We bring here some of the results we found in [9] to show the effects of m , q and d on EoP and CoP. The figures in this section are also from our previous work, reference [9].

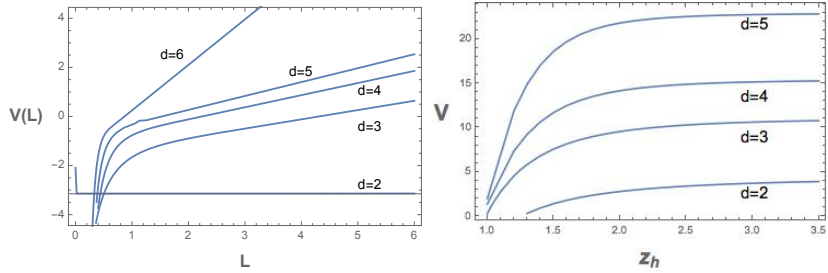


Figure 2. The volume $V(L)$ corresponding to each length of strip with the width L , for various dimensions d .

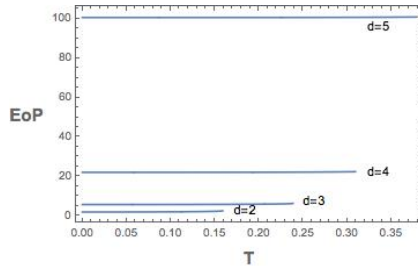


Figure 3. The EoP curves for different dimensions are shown here. For both cases we took $l = 20$ and $D = 0.3$.

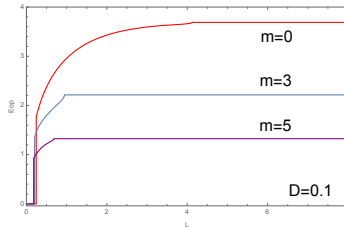


Figure 4. EoP as a function of l with $D = 0.1$.

As you could see from the figures, in [9], we actually noticed that in the case of massive gravity where the graviton has a small mass, EoP/CoP would decrease.

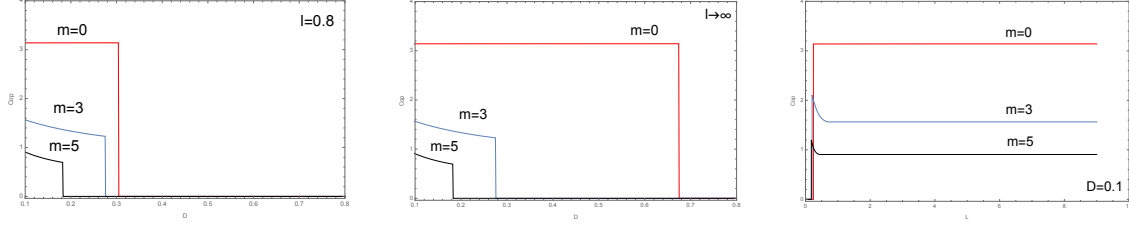


Figure 5. The CoP as a function of D with $l = 0.8$ (left) and $l = \infty$ (middle), and CoP as a function of l with $D = 0.1$ (right) is shown here.

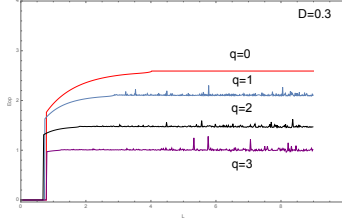


Figure 6. The relationship between EoP and l with $D = 0.3$.

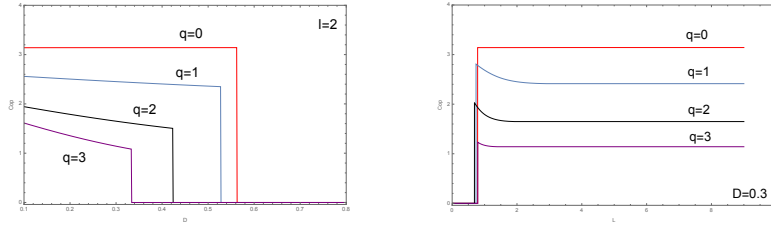


Figure 7. The relationship between CoP and l with $D = 0.3$.

We therefore expect to see this decreasing effects in particular stages and formulas of bulk reconstruction methods, such as tensor networks, modular Berry connection and quantum error corrections which is one of the motivations of this work.

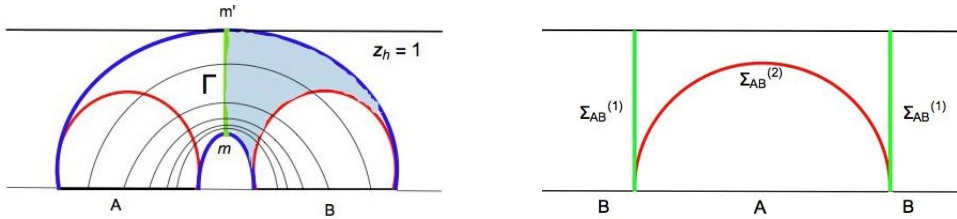


Figure 8. The modular flow and edge modes along the minimal wedge cross section could be studied to depict the relation between the flow of modular zero-modes, the holonomy which they create and their effects on EoP and CoP of mixed states.

In [9], we also found that the correlation strengths and density of bit threads would have a decreasing behavior along Γ from the turning point m toward the turn-

ing point m' . We would like to check this observation using other bulk reconstruction methods as well. For instance we could show that modular zero modes would have a decaying behavior along this path.

We give a short overview of modular Hamiltonian and modular Berry phase, quantum recovery channels and the connections between them and then we study these procedures in our setup and the effects of the parameters we are interested in, on the formulations of bulk reconstruction.

3 Entanglement Wedge Cross Section and Modular Flow

One of the main question of holography is that using the subregion duality, how from the operator algebra of boundary CFT, the physics of bulk entanglement wedge would emerge. One of guiding principles would be a duality found in [17], connecting the entanglement of purification between mixed states and the area of the minimal entanglement wedge cross section, i.e, the $E_W = E_P$ conjecture.

This duality would have connections with the behavior of modular zero-modes and modular Hamiltonian of [6–8]. We would like to connect $E_W = E_P$ conjecture to the setup of [6] using the duality between the modular Hamiltonians of both sides within the code subspace, as the JLMS formula [18]

$$H_{\text{mod}}^{\text{CFT}} = \frac{A}{4G_N} + H_{\text{mod}}^{\text{bulk}} + \dots + O(G_N). \quad (3.1)$$

In this relation, the modular Hamiltonian is defined as $H_{\text{mod}} = -\log \rho$, and A is the area operator of HRRT surface. The gravity dual of modular Hamiltonian operators also has been discussed in [19]. For a fixed spatial region R , modular Hamiltonian could be written as

$$H = -\log \rho_R \otimes I, \quad (3.2)$$

and the modular evolution of a density matrix ρ could be written as

$$\rho_\alpha \equiv e^{-i\alpha H} \rho e^{i\alpha H}. \quad (3.3)$$

Note that H is a state-dependent operator and also due to a kink at the boundary of R , it would be non-smooth. However, the full modular Hamiltonian for a region V which could be written as

$$\hat{H}_V = H_V - H_{\bar{V}}, \quad (3.4)$$

would be smooth, [19], as it has support on all regions of space. Also, it always annihilates the vacuum, $\hat{H}_V |0\rangle = 0$. In [20], it has been shown that it could be written in terms of energy momentum tensor in the form

$$\hat{H}_\gamma = 2\pi \int d^{d-2}x^\perp \int_{-\infty}^{\infty} d\lambda (\lambda - \gamma(x^\perp)) T_{\lambda\lambda}(\lambda, x^\perp). \quad (3.5)$$

So the general form of modular Hamiltonian for a region A could be written as

$$H_A = \int_A d\sigma^\mu T_{\mu\nu} \eta^\nu, \quad (3.6)$$

where η^ν is a time-like vector that generates the modular flow for the region A .

Note that based on the perspective of [18], the bulk and boundary modular flows and the relative entropies in the bulk and boundary are dual to each other.

The question would be using this duality, and also intuitions from other formalisms such as tensor network and bit thread picture, we check how these new ingredients such as zero-modes, edge modes and other normal modes would behave along the surface Γ and how they could actually glue together the entanglement wedge of each boundary CFT, as they are correlated and forming a mixed state, and then how they could reconstruct the curvature of the metric in the bulk.

From the intuitions of bit thread, tensor network and $E_W = E_P$ conjecture we claim several statements here.

First, note that the recent studies in [6] were focused on edge modes along HRRT surface. Here, as we study the correlations for mixed states and the connections between modular flow, CoP and EoP, we should focus our studies on not only the zero-modes, but the flow of the whole “normal modes”, and not just along HRRT surface but along the “*minimal wedge cross section*” between the two mixed CFTs.

Note that while expanding the quantum fields, where each term is a c-number valued function of spacetime, one would have *both* the zero and normal modes where each would multiplied by the corresponding operator. We claim that, while the operators for zero-modes would play the special role, all other modes would be necessary to construct the geometry of the bulk with mixed states. Note that the new “*collective degrees of freedom*” of instanton would deform the background and changes the *t'* Hooft interactions.

Alternatively, one could imagine that the collective degrees of freedom for all bit threads connecting qubits in the two regions would be along the minimal wedge cross section Γ as for two symmetric boundary regions, the center of “mass” of these threads lie on Γ . Considering these pictures, our first result would be

*Claim: Through the entanglement wedge cross section, the maximum amount of flow of **edge modes** [21] would pass.*

The flow of these modes could be actually formulated using amplitude of wavefunction between states on A and B as $\langle \phi_A | e^{-\pi K_A} \mathcal{J} | \phi_B \rangle$ where K_A is related to modular Hamiltonian and would implement the CPT transformation $\mathcal{J} : H_B \rightarrow H_A$. Also, the operator K_A in a special case where the angular coordinate θ around the entangling surface is zero, could be written as

$$K_A = \int_A d^{D-1}x f(x) T_{00}, \quad (3.7)$$

where T_{00} is the energy density and $f(x)$ is a weight function. So on Γ , this weight function, make the amplitude of transformation maximum. We will get back to more studies of modular zero modes along Γ later in future sections.

The second claim is:

*Claim: The pattern of **entanglement of purification** between mixed boundary CFTs would create the bulk curvature. As MI and EoP have decreasing gradient along the surface Γ , the bulk would be negatively curved.*

Then, the next claim involve the structure of modular Hamiltonian and modular zero modes using the structure of [6], which we explain the structure later. But the main point, is the role of minimal entanglement wedge cross section in the argument and how $E_P = E_W$ gives intuitions about the structure of bulk curvature coming from two mixed boundary regions.

Claim: When in our setup, one jumps from the HRRT surface with turning point m to the HRRT surface with turning point m' , the change in the local gauge and the modular Hamiltonian, would be proportional to the area of minimal wedge cross section Γ .

So the structure of entanglement of purification and the connections between the algebra of the two Hilbert space of *mixed states* would dictate the structure of bulk curvatures. For instance, similar to [6], one could imagine that for each pair of qubit on the two subregions A, B , a map between two Hilbert space would transform under the action of a local $SU(2)$ symmetry as

$$|i\rangle_A \rightarrow |\tilde{i}\rangle_B = \sum_j = W_{ij} |j\rangle_B, \\ W_{ij} \rightarrow U_{A,ik}^\dagger W_{kl} U_{B,lj}. \quad (3.8)$$

The matrix W_{ij} could be considered as Wilson loops between the two regions connecting qubits on each side. Based on the idea of $ER = EPR$, each of these would be a wormhole connecting the qubits. Now the pattern of “*Entanglement of Purification*” would dictate the local density of threads and their gradient along the surface Γ , moving from turning point m to m' .

Then we have the following picture,

Claim: As the correlations between pairs in the two subregion are stronger when they are closer to each other, the density of threads would be higher around those points, (also the gradients of change of correlations would be higher), the densities of bit threads, modular flow and edge modes are bigger around m , the holonomy is bigger around the point m compared to m' , the density of the symmetry operators or symmetry generators is higher, the Bures metric has a bigger absolute value and also the curvature in the bulk is bigger around the HRRT surface associated to turning point m compared to the one passing from m' .

These claims could actually indicate that the gradient of modular flow would be similar to the behavior of bit threads, or even a gradient of an electric field between

two charged strips, as the flow between two equal and symmetric strips would be symmetric and decreasing moving further away from the strips along Γ , as shown in figure 8. Also, we expect that similar to bit threads formalism, the modular flow has a bound of $J \leq \frac{1}{4G_N}$ which actually has been observed in [22] too.

So, the gradient of bit threads could be found by considering the behavior of modular scrambling modes around various RT surface along the minimal entanglement wedge cross section. In a dynamical setup, the change in modular Hamiltonian of the boundary region (for instance by closing the two strips to each other in our case), would act as a vector flow close to RT surface which would depend on the boost vector and gradient of fields in the bulk.

Then, the effects of varying physical parameters of the boundary system, on the bulk reconstruction, through modular Hamiltonian and modular flow, could be studied and check how these parameters would also affect minimal wedge cross section in the bulk, by changing EoP and CoP and the patterns of correlation in the boundary.

We conjecture that parameters such as mass of graviton m or charge of the system, q , would decrease the growth of the “code subspace” of the matrix elements of modular flow rate of change, $\delta H_{\text{mod}}(s)/\delta s$, and bring the bound lower than 2π . As the mass of graviton is dual to the viscosity parameter in the field theory side, one would expect that increasing this parameter would damp the “modular scrambling modes” which in fact are related to the modular Hamiltonian instead of the usual Hamiltonian of the system.

The change in the modular Hamiltonian of the system due to the viscosity and dissipations could be understood by considering the change in the energy momentum tensor. The energy momentum tensor in terms of the viscosity coefficients could be written as [23]

$$T^{\alpha\beta} = \rho u^\alpha u^\beta + q^\alpha u^\beta + q^\beta u^\alpha + (p - \zeta\Theta)h^{\alpha\beta} - 2\eta\sigma^{\alpha\beta}, \quad (3.9)$$

where ρ is the energy density, u^α is the velocity of the “comoving” observer and q^α is the spacelike “heat” flux vector that satisfy $q^\alpha u_\alpha = 0$. Also, we have $\zeta > 0$ and $\eta > 0$ which they are the bulk and shear viscosity respectively. The parameter $\Theta = u^\alpha_{;\alpha}$ is the expansion and also $\sigma^{\alpha\beta}$ is the shear tensor which is

$$\sigma^{\alpha\beta} = \frac{1}{2} \left(u^\alpha_{;\mu} h^{\mu\beta} + u^\beta_{;\mu} h^{\mu\alpha} \right) - \frac{1}{3} \Theta h^{\alpha\beta}. \quad (3.10)$$

In fact, the stress tensor could be written as the sum of three terms as [23]

$$T^{\alpha\beta} = T_{pf}^{\alpha\beta} + T_{heat}^{\alpha\beta} + T_{visc}^{\alpha\beta}, \quad (3.11)$$

where

$$T_{pf}^{\alpha\beta} = \rho u^\alpha u^\beta + p h^{\alpha\beta}, \quad T_{heat}^{\alpha\beta} = q^\alpha u^\beta + q^\beta u^\alpha, \quad T_{visc}^{\alpha\beta} = -\zeta\Theta h^{\alpha\beta} - 2\eta\sigma^{\alpha\beta}. \quad (3.12)$$

From these relations, one could see that the mass parameter m can increase the coefficients ζ and η and therefore, decreases the matrix elements of energy momentum tensor and also their derivatives, leading to the damping of the modular scrambling modes, and modular chaos modes. Also, the same charge of the system, because of the repulsion between the internal degrees of freedom, could lead to the suppression of the modular scrambling modes and modular chaos.

One may actually be able to calculate the modular Hamiltonian and the growth rate of modular flows, in the presence of these additional parameters such as charge and mass directly and prove this conjecture. The modular Hamiltonian and modular chaos bound could be calculated for dissipative systems using some field theory models as those introduced in [24]. Their structure could model dissipative systems with gapped momentum states using the two-field Lagrangian. Using this model, then one can test how the modular chaos bound would decrease from the maximum value of 2π , by a factor proportional to the dissipation parameter $\tau = \frac{\eta}{G}$, where here η is the viscosity and G is the shear modulus. Note that due to the dissipations, the theory would be non-Hermitian here.

Also, in these systems, due to the dissipation, the correlation functions show decaying oscillatory behaviors. However, we expect that, in these mixed decaying systems, the JLMS relation [18]

$$\langle \chi_i | H_{\text{mod}}^{CFT} | \chi_j \rangle = \langle \chi_i | H_{\text{mod}}^{\text{bulk}} | \chi_j \rangle, \quad \forall |\chi_i\rangle \in \mathcal{H}_{\text{code}}^\psi, \quad (3.13)$$

would still work.

In addition, for the connections between the modular flowed operators in each regions of A or B , and the correlations between the bulk fields on RT surfaces and operators on each boundary region part, the result of [4] could be extended to our mixed setup of figure 1 and we could get the following relation for our setup,

$$\begin{aligned} \int_{-\infty}^{\infty} ds \rho_R^{-is/2\pi} O(x_A) \rho_R^{is/2\pi} &= 4\pi \left[\int_{\partial r_A} dY_{RT_A} \langle \Phi(Y_{RT_A}) O(x_A) \rangle \Phi(Y_{RT_A}) \right. \\ + \int_{\partial r_B} dY_{RT_B} \langle \Phi(Y_{RT_B}) O(x_A) \rangle \Phi(Y_{RT_B}) &- \int_{\partial r_C} dY_{RT_C} \langle \Phi(Y_{RT_C}) O(x_A) \rangle \Phi(Y_{RT_C}) \\ \left. - \int_{\partial r_D} dY_{RT_D} \langle \Phi(Y_{RT_D}) O(x_A) \rangle \Phi(Y_{RT_D}) \right], \end{aligned} \quad (3.14)$$

which we have used the relation 2.2 for mutual information between A and B , i.e, $I = 2S(l) - S(D) - S(2l + D)$, and the result of [4] and specifically their equation 1.6, to write the above relation. Note that RT_A is the RT surface for only region A , RT_B is the RT surface for only region B , RT_C is the RT surface for the part D which passes from the point m , and RT_D is the RT surface for the part $2l + D$ which passes through the point m' .

The structure of zero modes in the mixed states could also be understood by writing the equation 4.33 of [4] for the mixed setups. Their result for a free theory

and for Gaussian states could be extended to our specific mixed setup as

$$\begin{aligned} \Phi_0(Z_X) &= 2 \int_{RT_A} \sqrt{h_{I_{RTA}}} dY \left(f_{\Pi}(Y)\Pi(Y) + f_{\Phi}(Y)\Phi(Y) \right) \\ &\quad - \int_{I_{RTC}} \sqrt{h_{I_{RTC}}} dY \left(f_{\Pi}(Y)\Pi(Y) + f_{\Phi}(Y)\Phi(Y) \right) \\ &\quad - \int_{I_{RTD}} \sqrt{h_{I_{RTD}}} dY \left(f_{\Pi}(Y)\Pi(Y) + f_{\Phi}(Y)\Phi(Y) \right), \end{aligned} \quad (3.15)$$

where h_i is the induced metric on I_i and also $\Pi = n^\mu \partial_\mu \Phi$. Using lattice models, the properties of these relations and the behavior of zero modes versus lengths l , D or dimension d could then be studied numerically.

Note that for the points close to the RT surfaces, as $Y \rightarrow Y_{RT}$, the modular flow of the operator would behave as

$$\lim_{Y \rightarrow Y_{RT}} f_{\Pi}(Y) = -2\pi \langle \Phi(Y_{RT}) \Phi(X) \rangle. \quad (3.16)$$

The bulk field could also be written in terms of the smearing function and the modular evolved modes as [4]

$$\Phi(X_R) = \int ds \int_R dx f_s(X|s) \mathcal{O}_s(x) = \int dw \int_R dx f_w(X|x) \mathcal{O}_w(x), \quad (3.17)$$

where f_w is actually a distribution function. This is a main formula for the entanglement wedge reconstruction which could still be used in mixed setup and also could be used for the studying the connections between modular flow and EoP and CoP.

3.1 Quantum recovery channels versus modular flows in mixed states

As we mentioned, both modular hamiltonians and quantum recovery channels could model the entanglement wedge reconstruction, so we would expect physical connections between them. One should note that both of these approaches would actually establish a map between the algebras that are localized in different subregions of the system.

The modular Hamiltonian has been used in constructing many holographic quantum measures such relative entropy and for bulk reconstruction. On the other hand, the main point of using a universal quantum recovery channel and quantum error correction formalism would be related to reconstructing information from damaged information, as some partial parts of the information of the system would be damaged due to the noise. As one would expect that modular evolution has memory, one could imagine that the damaged information are still encoded in the modular flow which could then be extracted, and therefore this signals the connection.

First, note that the classical channel is a conditional probability distribution $\{p_{Y|X}(y|x)\}_{x \in \mathcal{X}, y \in \mathcal{Y}}$, where X is the input system and Y is the output system which

acts over the alphabet \mathcal{X} and \mathcal{Y} . Then, the reversal channel could then be written as [25]

$$p_{X|Y}(x|y) = \frac{p_X(x)p_{Y|X}(y|x)}{\sum_x p_X(x)p_{Y|X}(y|x)}. \quad (3.18)$$

A “quantum” channel \mathcal{N} is also a completely positive, trace-preserving quantum “map”. It would be reversible if there would be another quantum channel \mathcal{R} , known as the recovery channel, which makes the composition $\mathcal{R} \circ \mathcal{N}$ to act as an identity in the form of $\mathcal{R} \circ \mathcal{N}[\rho] = \rho$.

The Petz map is specifically an example of recovery channel which is a quantum generalization of this reversal channel, and is a function of the quantum channel \mathcal{N} . The quantum channel \mathcal{N} is the generalization of the classical map $p_{Y|X}(y|x)$. Also, the input state to the channel, σ , is the generalization of $p_X(x)$.

The Petz map could also be written as

$$\mathcal{P}_{B \rightarrow A}^{\sigma, \mathcal{N}}(\omega_B) := \sigma_A^{1/2} \mathcal{N}^\dagger(\mathcal{N}(\sigma_A)^{-1/2} \omega_B \mathcal{N}(\sigma_A)^{-1/2}) \sigma_A^{1/2}, \quad (3.19)$$

which is a function of the quantum state σ_A and the quantum channel $\mathcal{N}_{A \rightarrow B}$ which takes system A to B . Also, ω_B is the input density operator. In another notation, it could also be written as

$$\begin{aligned} \mathcal{O}_R &= \sigma_R^{-\frac{1}{2}} \text{Tr}_B(\mathcal{O}) \sigma_R^{-\frac{1}{2}}, \\ \sigma_R &= \text{Tr}(\Pi_{\text{code}}) = \sum_{a=1}^{d_{\text{code}}} = \text{Tr}_B(|\Psi_a\rangle \langle \Psi_a|). \end{aligned} \quad (3.20)$$

In fact, Petz map is the composition of three completely positive (CP) maps which would lead to an indirect procedure for the bulk reconstruction.

In [10], the *twirled Petz map* has been written as

$$\mathcal{R}_{\sigma, \mathcal{N}} := \int_{\mathbb{R}} dt \beta_0(t) \sigma^{-\frac{it}{2}} \mathcal{P}_{\sigma, \mathcal{N}}[\mathcal{N}[\sigma]^{\frac{it}{2}}(\cdot) \mathcal{N}[\sigma]^{-\frac{it}{2}}] \sigma^{\frac{it}{2}}, \quad (3.21)$$

where $\mathcal{P}_{\sigma, \mathcal{N}}$, is the normal *Petz map* as

$$\mathcal{P}_{\sigma, \mathcal{N}} = \sigma^{1/2} \mathcal{N}^*[\mathcal{N}[\sigma]^{-1/2}(\cdot) \mathcal{N}[\sigma]^{-1/2}] \sigma^{1/2}, \quad (3.22)$$

and \mathcal{N}^* is the adjoint of channel \mathcal{N} . Also β_0 is the probability density which is $\beta_0(t) := \frac{\pi}{2} (\cosh(\pi t) + 1)^{-1}$. For bulk reconstruction, both of these could be used, so the connection between modular Hamiltonian and quantum recovery channel could be traced using both of these formulation.

In [26], it has been shown how to construct a recovery channel $\mathcal{R} : S(\mathcal{H}_B) \rightarrow S(\mathcal{H}_A)$ from any reversible channel $\mathcal{N} : S(\mathcal{H}_A) \rightarrow S(\mathcal{H}_B)$, where \mathcal{H}_A and \mathcal{H}_B are

two Hilbert spaces. Note that any recovery channel would act approximately as $\mathcal{R} \circ \mathcal{N}[\rho] \approx \rho$, $\forall \rho \in \mathcal{S}(\mathcal{H})$, so it should be able to reconstruct the original density matrix with sufficient precision. Since the quality of this approximation would depend on the behavior of relative entropy under the action of the channel \mathcal{N} [10], then, from the connections between relative entropy and modular Hamiltonian, the connection between the quantum recovery channel and modular flows could just be noticed right here.

Also, when the two subsystems in our setup become closer to each other, the noise would get greatly increased as more information would be damaged. Then, from the modular Berry flow point of view, one could check that the flows would become more chaotic.

One important aspect is the monotonicity of the relative entropy which would indicate that by acting any quantum channel \mathcal{N} , the relative entropy between two states would never increase, so we have

$$D(\rho|\sigma) \geq D(\mathcal{N}[\rho]|\mathcal{N}[\sigma]), \quad (3.23)$$

where again $D(\rho|\sigma) := \text{Tr} \rho \log \rho - \text{Tr} \rho \log \sigma$ is the relative entropy between ρ and σ .

The approximate version developed in [27], is as follows

$$D(\rho|\sigma) - D(\mathcal{N}[\rho]|\mathcal{N}[\sigma]) \geq -2 \log F(\rho, \mathcal{R}_{\sigma, \mathcal{N}} \circ \mathcal{N}[\rho]), \quad (3.24)$$

where $F(\rho, \sigma) := |\sqrt{\rho} \sqrt{\sigma}|_1$ is the fidelity. This inequality then put a constraint on the holographic bulk curvatures and modular chaos modes. It worths to mention here that the parameters such as dissipation, quantified by the mass of graviton m , or parameters such as the same-sign charge of the system q , would make the term $F(\rho, \mathcal{R}_{\sigma, \mathcal{N}} \circ \mathcal{N}[\rho])$ smaller, as the recovery channel works with less precision.

Another connection between the modular Hamiltonian and quantum recovery channel in the bulk reconstruction could be derived by combining the results of [10] and [22]. In [10], it has been shown that a boundary operator could be computed as the response of the modular Hamiltonian of the specific subregion to a perturbation of the average code state, which is in the direction of the bulk operator. In another word, a bulk operator could be considered as the response of the boundary region's modular Hamiltonian to a perturbation of the bulk state in the direction of the bulk operator which would be the noncommutative version of Bayes' rule and has a representation in terms of modular flows. We aim to check what this recovery channel would tell about the minimal wedge cross section and the modular flow through it.

So for all the bulk operators ϕ_a , with support in the entanglement wedge a , we have

$$\mathcal{O} := \mathcal{R}^*[\phi_a] = \frac{1}{d_{\text{code}}} \int_{\mathbb{R}} dt \beta_0(t) e^{\frac{1}{2}(1-it)H_A} \text{Tr}_{\bar{A}} [J(\phi_a \otimes \mathbb{1}_{\bar{a}}) J^\dagger] e^{\frac{1}{2}(1+it)H_A}, \quad (3.25)$$

where $H_A = -\log(J\tau J^\dagger)_A$ is the boundary modular Hamiltonian on subregion A which is associated with the maximally mixed state τ on the code subspace.

In other way, it could be written as the logarithmic directional derivative as

$$\mathcal{O}_A = \mathcal{R}^*[\phi_a] = -\frac{1}{d_{\text{code}}} \frac{d}{dt} \Big|_{t=0} H_A[\tau_{\text{code}} + t\phi_a \otimes \mathbb{1}_{\bar{a}}]. \quad (3.26)$$

As in [22], a bound on the infinitesimal perturbation of the modular Hamiltonian have been derived, one could then put a constraint on the perturbative effects of the quantum channel, since we have $dH_{\text{mod}} \propto (d\tau_{\text{code}} + ds(\phi_a \otimes \mathbb{1}_{\bar{a}}))$ and we get the following bound

$$\left| \frac{d}{dt} \Big|_{t=0} \log \langle \chi_j | (J(\tau_{\text{code}} + t\phi_a \otimes \mathbb{1}_{\bar{a}})J^\dagger) | \chi_j \rangle \right| \leq \frac{2\pi}{d_{\text{code}}}. \quad (3.27)$$

This means that the boundary operator which corresponds to ϕ_A is related to the response of acting the boundary modular Hamiltonian H_A to a perturbation of the maximally mixed code state in the direction of the operator ϕ_a . So the connection has been further established and also this new bound has been found. We also expect that having the maximum modular flow through the minimal entanglement wedge cross section would correspond to the most efficient quantum error correction codes, which we later explain it in more details.

It worths mentioning here that the relation 3.27, could also specify the bound on the maximum density of bit threads along the minimal entanglement wedge cross section in our setup of two intervals for such mixed state.

In [25], also the connections between Petz recovery channels and pretty good measurements have been discussed. Additionally, using pretty good measurements which is a special case of Petz recovery channel, the various indications of the connection could be studied. This channel could actually allows for near-optimal state discrimination. The error probability of pretty good measurement (PGM) would be

$$P_e^{\text{PGM}} \leq \sum_{i \neq j} \sqrt{p_i p_j} F(\sigma_i, \sigma_j), \quad (3.28)$$

where $\{\sigma_i\}$ is a set of density matrices and p_i is the probability that a quantum state ρ is in state σ_i and F is the fidelity function. As the fidelity and complexity are proportional [28], using volume complexity, this inequality then could put a bound on PGM which is special case of Petz map. Therefore, quantities such as capacity of quantum recovery channels would also be bounded by complexity. Also, using the gradient of modular flow, the compressibility of quantum messages and also the capacity of quantum channels could be estimated.

Another important observation is that the bound on quantum error correction for every channel Λ as

$$\min_{|\psi\rangle \in \mathcal{C}^{\otimes 2}} \max_{\mathcal{D}} \langle \psi | (\mathcal{D} \circ \Lambda \otimes I)(|\psi\rangle \langle \psi|) | \psi \rangle \geq 1 - \epsilon, \quad (3.29)$$

would be related to the bound on modular Hamiltonian

$$\|e^{-iH_{\text{mod}}s}e^{i(H_{\text{mod}}+\epsilon\delta H_{\text{mod}})s}\| \leq 1, \quad (3.30)$$

for the strip $-\frac{1}{2} \leq \text{Im}[s] \leq 0$ strip. This indicates the connections between the upper bound on the changes of the modular scrambling modes and the maximum precision of quantum error correction.

Next, the relations between quantum error corrections and chaos could be used. In [29], the connections between chaos, eigenstate thermalization hypothesis (ETH) and quantum error correction have been discussed. The eigenstate thermalization hypothesis could be written in the form

$$|\langle E_l | O | E_l \rangle - \langle E_{l+1} | O | E_{l+1} \rangle| \leq \exp(-c_1 N), \quad \text{and} \quad |\langle E_k | O | E_l \rangle| \leq \exp(-c_2 N), \quad (3.31)$$

where $c_1, c_2 > 0$ are two constants and E_l are the energy eigenstates.

The constraint on the modular scrambling mode growth rate would be related to the approximate version of the Knill-Laflamme condition in the form of

$$\langle \psi_i | E | \psi_j \rangle = C_E \delta_{ij} + \epsilon_{ij}, \quad (3.32)$$

where the index i is for the codewords that span the code space in the form $\mathcal{C} = \text{span}(\{|\psi_1\rangle, \dots, |\psi_{2^k}\rangle\})$. Then, the error in 3.29 would have the bound as $\epsilon \leq 2^{2(k+d)}$ where also d is the number of qubits in the system.

So by increasing d , the system size, the total error would decrease and one could achieve the initial state with a higher probability, close to 1. For the modular Hamiltonian, this also has the implication that by increasing the system size, modular zero modes would increase, which would lead to a smoother bulk geometry, and also the bound 3.30 would get closer to 1 as well. Therefore, the connections between quantum error correction, chaos, and modular chaos could be seen from ETH.

All in all, one could say that considering "all" the modular flows, passing through entanglement wedge cross section, corresponds to a "perfect" quantum error correction where

$$(\mathcal{R} \circ \mathcal{N})[\rho] = \rho \quad \text{for all} \quad \rho \in S(\mathcal{H}_A), \quad (3.33)$$

and where the quantum channels are maps as $\mathcal{N} : S(\mathcal{H}_A) \rightarrow S(\mathcal{H}_B)$ and $\mathcal{R} : S(\mathcal{H}_B) \rightarrow S(\mathcal{H}_A)$.

Note that the mixed quantum systems which have a connected bulk geometry, which also satisfy ETH, would have a richer family of eigenvalues as well, and so these form a bigger approximate quantum error correction codes (AQECC). Even the AQECC for the connected versus two disconnected bulk systems, under different errors, would perform differently, and so these even would be able to detect the phase transitions.

The difference between the codes in the disconnected and connected cases could also be further understood by considering the theorem 1 of [29]. If we imagine that in each strip we could implement N sites, for each case, in the initial state, we would have a set of energy eigenvalues close to \mathbf{E}_1 where $S_{\mathbf{E}_1} := \{E_k : E_k \in \mathbf{E}_1 - \sqrt{N}, \mathbf{E}_1 + \sqrt{N}\}$. Then, when the two strips get close enough where the mutual information and EoP get non-zero, the sets of energy eigenvalues become mixed, and a bigger set which its components are close to \mathbf{E}_2 as $S_{\mathbf{E}_2} := \{E_j : E_j \in \mathbf{E}_2 - \sqrt{2N}, \mathbf{E}_2 + \sqrt{2N}\}$ would take shape. Since there would be more eigenstates and the distance between them would become smaller, the error of AEQCC would become smaller too. In this case the distance of the code would change as $\Delta \sim \log(2)$.

When the two subregions are far from each other and the mutual information between them is zero, in each region, the eigenstates which have close energies, would form an approximate quantum error correcting code (AQECC) which all together reconstruct their own corresponding bulk dual space. When the two regions become close enough to each other, more eigenstates would be available and the ones from each region could form more AQECCs, and even between the two subregions, and therefore the dual “connected” entanglement wedge in the bulk would be constructed.

There are two reasons one would expect the discussion of [29] would work for the mixed setup and connected entanglement wedge reconstruction. One is the invariance of states under modular flow for any subregion, which could be written as $\delta H_{\text{mod}} |\psi\rangle = 0$ or $G_{\pm} |\psi\rangle \approx 0$. This would lead to the approximate local isometries of $\mathcal{L}_{\zeta(\pm)} g_{\mu\nu}(x^\alpha = 0, y^i) = O(e^{-2\pi\Lambda})$ along all the RT surfaces and even those connecting the two regions [22]. In fact the existence of this symmetry could ensure the “uniformity” of spreading of information along the the minimal wedge cross section Γ , and so this fact again reassures us that even after mixing, the code would not be corrupted by noise completely and is still capable of bulk reconstruction.

The other point is the finiteness of the correlation length, which even in the mixed setup still ensures that the spreading of information would not diverge and just be uniform enough to form a nice bulk geometry from the mixed correlations.

Another interesting point on the effect of charge comes from studying the connections between quantum error correction and holography. For instance, note that in [30], where they studied the approximate error correction in the presence of continuous symmetries and Haar-random charged systems, a bound on the recovery error has been found as error $\gtrsim \frac{Q}{n}$ where Q is the total charge of the state and n is the number of physical subsystems where the system is made of. So one could see that by increasing the charge Q , the minimum error for constructing states would increase so for the bulk reconstruction, less quantum recovery channels and fewer gates would be needed and therefore once again one could see that charge would decrease the complexity of purification.

We could get further connections from other symmetry generators. The observation in [22], is that the chaotic properties of the dual boundary CFT theories

would lead to the symmetry generators in the bulk. Near the RT surfaces in the bulk, as found in [22], the modular Hamiltonian would act as a geometric boost, i.e, $[\delta H_{\text{mod}}, \phi(x^\alpha, y^i)] \propto 2\pi \left(\zeta_{(+)}^\mu - \zeta_{(-)}^\mu \right)$. So the zero modes close to RT surfaces have translation invariant. If the ETH would be applicable in the system too, then using the result of [29], for the $2d$ case one could show that an AQECC would hold. This result then indicates more relationship between modular chaos and quantum error corrections. The formation of quantum error correcting codes (QECC) in chaotic systems which eigenstates exhibit the eigenstate thermalization hypothesis is related to the saturation of modular scrambling modes, so one expects that quantum recovery channels would also satisfy the relations of [22], found for modular chaos.

As ETH have many significant implications for QECCs, its implications for EoP and CoP would be significant too. The dynamical properties could also point out to other connections. For instance, in [31], the fluctuation theorem has been applied to quantum recovery channels. Their complex-valued entropy production could detect the relation between the forward and backward processes through the quantum channel. So, one could propose that the imaginary part of our complexity of purification is actually related to the symmetry breaking while passing through the quantum channel.

By changing the parameters of the system, further connections could be revealed. For example, the parameter m increases the dissipations in the channel and therefore decreases the correlations among the two subregions. In this case, then less modes could pass through the quantum recovery channels and so increasing m would decrease the imaginary parts of entanglement and complexity of purification as we observed in [9]. The same argument would apply for the case where the two subregions have a same sign charge q . We could then propose that these two quantities increase the errors in AQECCs, would suppress the flow of modular modes, and so decrease EoP and CoP.

Now we could investigate the relations for the modular zero modes and the connections with EoP and CoP in more details. For each subsystem, the zero modes are those operators Q_i^A which satisfy the following relation

$$[Q_i^A, H_{\text{mod},A}] = 0, \tag{3.34}$$

where i indexes the zero-mode subalgebra. Due to the equivalence between bulk and boundary modular flows [18], for holographic CFTs which satisfy 3.34, the dual Bulk operators would be on the RT surfaces which are anchored on λ .

We should specify how the correlation functions “outside” of a CFT subregion A would change under the unitary evolution which are generated by modular zero modes Q_i^A . If all the correlation functions stay *within* the subregion A , then the evolution is invariant as we have the relation 3.34.

However, since here we are interested in understanding how the correlation functions and their relative bundles connect the subregion A to another region B in the

mixed state, this relation should be modified for the case of entanglement of purification. We expect that for the full setup of EoP, one would need to consider there, the whole normal modes and not just the zero modes.

So, for the mixed setup, we expect the commutative relations would be more complicated. For the case where the distance between the two subsystems is bigger than the critical distance, i.e, $D \geq D_c$, the mutual information is zero, $I = 0$ and therefore EoP = 0. In this case, for each of the two systems of A and B , we would still have $[Q_i^A, H_{\text{mod},A}] = 0$ and $[Q_i^B, H_{\text{mod},B}] = 0$. However, for $D \leq D_c$ when the two systems become correlated, we have non-zero commutations, i.e., $[Q_i^A, H_{\text{mod},A}] \neq 0$, $[Q_i^B, H_{\text{mod},B}] \neq 0$, $[Q_i^A, H_{\text{mod},B}] \neq 0$, $[Q_i^B, H_{\text{mod},A}] \neq 0$, which their values would depend on the amount of mixing and correlations between the subsystems, or actually the mutual information shared among them, and therefore on the parameters such as l , D , d , etc, which totally could be quantified by a mixing parameter μ which we later study. Note that, here, Q_i^A or Q_i^B are actually the generators of the unitary evolutions. For the whole system and for the modular Hamiltonian of the total system though, we expect that again the commutation relation would vanish.

Looking for more connections, we could turn to the studied of [6], where it was suggested that the modular Hamiltonian could be written as $H_{\text{mod}} = U^\dagger \Delta U$, where Δ has the information of the spectrum and the unitary operators U have the information of the basis of the eigenvectors. Then, its derivative with respect to the modular parameter λ could be written as

$$\dot{H}_{\text{mod}} = [\dot{U}^\dagger U, H_{\text{mod}}] + U^\dagger \dot{\Delta} U, \quad (3.35)$$

where we expect that this relation could work for the case of mixed setup as well.

Now the main question we would like to ask here is again how changing the charge q , or the dissipation rate, i.e, the parameter m would change each term in this relation as we would like to understand better the connections between the procedure of quantum recovery channels in entanglement wedge reconstructions and modular flow by studying the effects of charge and dissipation rate on each method.

For studying this problem, similar to [32], we could consider an out-of-time-order correlator (OTOC), but for the modular Hamiltonian, and in the setup of mixed states. So instead of the zero modes Q_0 , we need the operators Q_x , which has support near the position x . Then, the OTOC would be

$$\mathcal{C}(x, s) = \frac{1}{2} \text{Tr} \rho^{\text{eq}} [H_{\text{mod}}(s), Q_x]^\dagger [H_{\text{mod}}(s), Q_x], \quad (3.36)$$

where ρ^{eq} would be a Gibbs state. Using this relation, the Lieb-Robinson bound in the setup of modular chaos could be considered and it could be connected to modular chaos bound.

To make the study simpler we can use the model of [32], where for the spin-1/2 chain of length L , the spreading operator could have been written in the basis of

4^L Pauli string operators \mathcal{S} which are actually some products of Pauli matrices on distinct sites. We could do the same here and write our modular Hamiltonian which controls the evolution of modular scrambling modes in a setup as

$$H_{\text{mod}}(s) = \sum_{\mathcal{S}} a_{\mathcal{S}}(s) \mathcal{S}. \quad (3.37)$$

So similarly we could consider the modular Hamiltonian as some string operators which by passing the modular time s , they grow in the spatial extent. Then, the OTOC would be zero at first, when the two subregion are far away from each other, but it becomes non-zero when the two subregion move toward each other. The effects of mass and charge on modular Hamiltonian and modular chaos modes could now easily be seen by considering their effects on these strings.

We expect that the modular Hamiltonian satisfy a type of conservation law. Its operator norm $\text{Tr}[H_{\text{mod}}^\dagger H_{\text{mod}}]$ should be conserved which leads to the fact that the total weight of these Pauli strings $\sum_{\mathcal{S}} |a_{\mathcal{S}}|^2$ would be conserved as well. So for the modular scrambling modes, similarly one could imagine a hydrodynamical spreading picture. Then, the effects of charge or dissipation could be observed by using this model and just by considering their effects on the string operators.

When the left and right systems become close enough to each other that we get $I \neq 0$ and $\text{EoP} \neq 0$, then the zero modes would mix with each other, and the strings or the Wilson lines between them would become screened. The dissipation and (same-sign) charge would actually shrink the string operators. The charge and dissipation also make the scrambling time shorter and also the term $U^\dagger \dot{\Delta} U$ in relation 3.35 would reach to its maximum value faster.

The connections between the zero modes of modular Hamiltonian, modular Berry connection and curvature in the bulk were worked out in [6]. Our similar proposal about their connections then could stated that passing of gravitational edge modes through the quantum recovery channels would build the Berry connection.

In [6], a projector operator into the zero modes, P_0^λ , has also been proposed which could separate the contribution of spectrum changing in relation 3.35. It could be written as

$$P_0^\lambda[V] \equiv \lim_{\Lambda \rightarrow \infty} \frac{1}{2\Lambda} \int_{-\Lambda}^{\Lambda} ds e^{iH_{\text{mod}}(\lambda)s} V e^{-iH_{\text{mod}}(\lambda)s}, \quad (3.38)$$

or

$$P_0^\lambda[V] \equiv \sum_{E, q_a, q'_a} |E, q_a\rangle \langle E, q_a| V |E, q'_a\rangle \langle E, q'_a|, \quad (3.39)$$

where $|E, q_a\rangle$ would be the simultaneous eigenstates of modular Hamiltonian H_{mod} and a set of commuting zero mode operators Q_a . Also, E is the eigenvalue of H_{mod} and q_a is the eigenvalue of Q_a .

We would like to raise here, the similarities between the procedure of applying the projector operator P_0^λ , quantum recovery channels and also the Wilson line formulations.

As mentioned, the quantum recovery channel

$$\mathcal{P}_{B \rightarrow A}^{\sigma, \mathcal{N}}(\omega_B) := \sigma_A^{\frac{1}{2}} \mathcal{N}^\dagger (\mathcal{N}(\sigma_A)^{-\frac{1}{2}} \tilde{\omega}_B \mathcal{N}(\sigma_A)^{-\frac{1}{2}}) \sigma_A^{\frac{1}{2}}, \quad (3.40)$$

is actually a combination of three maps [25],

$$\begin{aligned} i) \quad & (\cdot) \rightarrow [\mathcal{N}(\sigma_A)]^{-1/2} (\cdot) [\mathcal{N}(\sigma_A)]^{-1/2}, \\ ii) \quad & (\cdot) \rightarrow \mathcal{N}(\cdot), \\ iii) \quad & (\cdot) \rightarrow \sigma_A^{1/2} (\cdot) \sigma_A^{1/2}. \end{aligned} \quad (3.41)$$

The combination of the first and third one is similar to applying the projection operator to zero modes. So we contemplate that the projector operator on to the zero-mode sector of $H_{\text{mod}}(\lambda)$ would actually act as a quantum recovery channel.

We would also like to bring up here the observation that the structure of Wilson line

$$U[x_i, x_f; C] = \mathcal{P} \exp \left(i \int_{\tau_i}^{\tau_f} d\tau \frac{dx^\mu}{d\tau} A_\mu(x(\tau)) \right) = \mathcal{P} \exp \left(i \int_{x_i}^{x_f} A \right), \quad (3.42)$$

would also be similar to the two other formulations of bulk reconstruction which could also act by itself as another method. In fact, all of these ideas are based on somehow similar multiple maps and projections.

Following our discussions on modular zero modes, note that the flux of zero modes along the minimal wedge cross section could be considered by the below integral

$$\int_m^{m'} dz \frac{d(U^\dagger \dot{\Delta} U)}{dz} \Big|_\Gamma = \int_m^{m'} dz \frac{d(P_0^\lambda [\dot{H}_{\text{mod}}(\lambda)])}{dz} \Big|_\Gamma. \quad (3.43)$$

So the change of spectrum of zero modes could also be written in terms of projection operator and rate of change of modular Hamiltonian. We could then write the spectrum complexity part of complexity of purification [9, 33] and its growth rate in terms of the above formula, where we explain further in section 3.2.

Note also that the mass parameter m and charge, would suppress the rate of growth spectrum complexity by suppressing the operators P_0 and \dot{H}_{mod} through the suppression of eigenvalues E and q_a .

One last point that we would like to mention in this section, is the connection between remaining in the code subspace along the minimal wedge cross section, which follows the equation

$$H_{\text{mod}} = P_{\text{code}} H_{\text{mod}}^{\text{exact}} P_{\text{code}}, \quad (3.44)$$

and staying within the distance smaller than D_c in our setup, where the mutual information is still non-zero, i.e, $I = S(l) + S(D) - S(2l + D) \neq 0$

We could argue that if the non-local effects outside the code subspace could be considered, the singularities of the first-order phase transitions noted in figure 5, could be removed. For instance, considering the effects of quantum tunnelings through the Berry potential, could improve the relation for the mutual information and remove the sudden drop in the figures of entanglement and complexity of purification and make those figures get vanish in late times smoothly. The quantum mutual information would satisfy the following inequality [34]

$$I(A, B) \geq \frac{\mathcal{C}(M_A, M_B)^2}{2\|M_A\|^2\|M_B\|^2}, \quad (3.45)$$

where $\mathcal{C}(M_A, M_B) := \langle M_A \otimes M_B \rangle - \langle M_A \rangle \langle M_B \rangle$ is the correlation function of M_A and M_B . So we could add the quantum effects to the mutual information, EoP and CoP and therefore remove the sudden drops.

Finally, we would like to remark that we expect $H_{\text{mod}}(\text{mixed})$ has more zero modes, and also when the system become mixed, the corresponding gauge groups would get larger. Also, we expect that for the mixed setup we have

$$[Q_i, P_{\text{code}} H_{\text{mode}(\text{mixed})} P_{\text{code}}] \neq 0. \quad (3.46)$$

Also, charge and dissipation (the term m) would definitely change the size and the behavior of projection operators and code subspace, where address these further in the next section.

3.2 Complexity, Berry phase and modular Hamiltonian

The question of what information modular phases yield could be answered now. In the setup of $\text{AdS}_3/\text{CFT}_2$, it has been shown in [8] that this point has actually connections with the entanglement and bulk reconstruction. We propose here that, in the bulk, modular phase is related to the complexity of purification introduced in [9].

For the case of AdS_3 , as we have seen CoP would be constant and its absolute value is exactly π . For higher dimensions, it wouldn't be constant and behaves similar to volume as shown in figure 2. It becomes much bigger as the dimension of space-times increase. This is similar to the behavior of Berry phase. Also, the behavior of EoP shown in figure 3, could show such connections between the correlations and modular Berry connection in various dimension. However, as we discussed, complexity and CoP would be better probes of correlations in mixed setup. Therefore, here we would like to find connections between CoP and Berry phase.

The initial aim of this section is to find the connections between Virasoro Berry phase and complexity of purification for mixed states. In [35], the connections between complexity measures in the path integral optimization proposal and Berry

phase have been depicted. Now here we would find more connections between the complexity of purification, basis complexity and spectrum complexity (defined in [33]), with the change of modular Hamiltonian.

As the modular Hamiltonian has been used in the calculations of relative entropy, entropy bounds, or determining statistical properties of vacuum CFTs, one would expect it would be useful in studying holographic computational complexity as well. In works such as [36, 37], it has been shown that the Berry curvature and Berry phase would also play an important role in studying many electronic properties in molecules and solids. The Berry's phases of the many-electron wavefunction have actually been related to several observable phenomena and measurable effects such as the polarization in the material, various manifestations of Hall effects, orbital magnetism and also quantum charge pumping. We here add to those studies by connecting Berry phase of many-body systems to complexity and complexity of purification. Specially, connections between quantum charge pumping, the direction of bit threads, the behavior of correlations between two mixed systems and purification would be related.

The modular Hamiltonian could be considered as the Hermitian operator on the CFT and can be decomposed as [6]

$$H_{\text{mod}} = U^\dagger \nabla U. \quad (3.47)$$

In the above relation ∇ is a diagonal matrix which determines the spectrum and as we will see, it would essentially be connected to the spectrum complexity. The unitary U specifies the basis of eigenvectors and it would be connected to the basis complexity.

From [6, 38], the relation 3.47, then leads to

$$\dot{H}_{\text{mod}} = [\dot{U}^\dagger U, H_{\text{mod}}] + U^\dagger \dot{\nabla} U, \quad (3.48)$$

where the dot is the derivative with respect to the quantity λ , $\dot{\cdot} \equiv \partial_\lambda$, which reparametrizes CFT.

In [6], the modular Berry connection is defined as

$$\Gamma(\lambda^i, \delta\lambda^i) = P_0^\lambda [\partial_{\lambda^i} U^\dagger U] \delta\lambda^i, \quad (3.49)$$

where P_0^λ is the projector which acts only on the zero-mode sector of $H_{\text{mod}}(\lambda^i)$. So we need to change it in a way that considers all the modes for using it for the EoP and CoP. So note that unlike the case in [6], in the mixed setups the transformation U would be generated not only by the zero modes but the whole modes as $U'_Q = e^{-i \sum_i Q'_i s_i}$ to connect A and B . Therefore, the form of H_{mod} for mixed states would not completely be preserved, but still the change in its form could be calculated and we propose would be related to complexity of purification.

Besides, we could connect the modular Hamiltonian to the definition of complexity of purification in [33] as the summation of two parts, basis complexity and spectrum complexity. As we have mentioned, the complexity of purification could be written as

$$CoP = \mathcal{C}_B + \mathcal{C}_s, \quad (3.50)$$

and in the boundary CFT, the change of modular Hamiltonian could also be decomposed into the change of basis and change of spectrum as [6]

$$\underbrace{\dot{H}_{\text{mod}}}_{\propto \text{CoP}} = \underbrace{[\dot{U}^\dagger U, H_{\text{mod}}]}_{\propto \mathcal{C}_B} + \underbrace{P_0^\lambda[\dot{H}_{\text{mod}}]}_{\propto \mathcal{C}_s}, \quad (3.51)$$

which then we could draw the connections between them from these relations.

The second part of 3.48, which corresponds to the change in the spectrum of modular Hamiltonian and therefore corresponds to spectrum complexity part of CoP could be written in the form of modular flow [6]

$$P_0^\lambda[V] \equiv \lim_{\Lambda \rightarrow \infty} \frac{1}{2\Lambda} \int_{-\Lambda}^{\Lambda} ds e^{iH_{\text{mod}}(\lambda)s} V e^{-iH_{\text{mod}}(\lambda)s}. \quad (3.52)$$

In the bulk, this relation could be written in the following form

$$\underbrace{\delta_\lambda \zeta_{\text{mod}}^M(x; \lambda)}_{\propto \delta \text{CoP}} = \underbrace{[\xi(x; \lambda, \delta\lambda), \zeta_{\text{mod}}(x; \lambda)]^M}_{\propto \text{rotation of the basis}} + \underbrace{P_0^\lambda[\delta_\lambda \zeta_{\text{mod}}^M(x; \lambda)]}_{\propto \text{change of spectrum}}. \quad (3.53)$$

These relations could show how the changes in modular Hamiltonian would change basis, spectrum and purification complexities. As one can see, the operator $\dot{U}^\dagger(\lambda)U(\lambda)$ corresponds to the basis component of complexity of purification and will turn the information corresponding to the infinitesimal shape variation.

We can also use these relations to define a first law of EoP as

$$\partial_\lambda \Delta \langle H_0 \rangle \Big|_{\lambda=\lambda_0} = \partial_\lambda \Delta \text{EoP}(A, \lambda) \Big|_{\lambda=\lambda_0}. \quad (3.54)$$

The gradient of EoP then could be written in term of the modular Hamiltonian as

$$\Delta \langle H_0 \rangle(A, \lambda) = \partial_\lambda \Delta S(A, \lambda) \Big|_{\lambda=\lambda_0} \tilde{\lambda} + \mathcal{O}(\tilde{\lambda}^2). \quad (3.55)$$

Note that entanglement entropy and relative entropy could also be written in terms of modular Hamiltonian as well. For instance, for a ball-shaped region A in the CFT, the first law of thermodynamics would be

$$\frac{d}{d\epsilon} (\langle H_A \rangle - S_A) = \frac{d}{d\epsilon} S(\rho_A || \rho_A^{(0)}), \quad (3.56)$$

where $\rho_A^{(0)}$ is the density matrix of region A without perturbation and $S(\rho_A||\rho_A^{(0)})$ is the relative entropy between the perturbed and unperturbed states.

Another example is the coherent states, where their modular Hamiltonian is equal to the canonical energy and also they would not change the bulk von Neumann entropy of subregion, as we have the relation $\Delta S_{\text{bulk}} = 0$ [18], which then would lead to

$$S_{\text{bdy}}(\rho||\sigma) = S_{\text{bulk}}(\rho||\sigma) = \Delta K_{\text{bulk}} - \Delta S_{\text{bulk}} = \Delta K_{\text{bulk}} = E_{\text{canonical}}. \quad (3.57)$$

So in the case of coherent states excitations, under the action of their specific quantum channel, modular Hamiltonian would not increase.

Additionally, the first law of entanglement entropy in terms of the modular Hamiltonian could be written as

$$\Delta S = S(\rho^1) - S(\rho^0) = \langle H \rangle_1 - \langle H \rangle_0 = \Delta \langle H \rangle. \quad (3.58)$$

Note that when the Hamiltonian of the system evolves adiabatically, the system would remain in the n -th eigenstate of the Hamiltonian, but it would gain a phase factor.

So, If we replace the Hamiltonian of the system with the modular Hamiltonian, similar to the studies of [6–8, 22], we could depict the connection between the Berry curvature and the modular scrambling modes but for the **mixed setup**. For doing that we could take into account the picture we got in [9] for the minimal wedge cross section, from the bit thread formalism.

Now if we consider the modular Hamiltonian for the evolution of the system (instead of the usual time evolution), we could consider the connections between modular Berry phase, modular Berry connection, and complexity growth of system. The varying modular Hamiltonian which is connected to the modular Berry phases, could also be calculated for the connected and disconnected cases, specially for the case where the two strips have unequal sizes.

When the modular evolution is cyclical, the modular Berry phase would be invariant and could be an observable of the system and the whole change could be characterized by this phase term.

Using the adiabatic approximation, the coefficient of the n th eigenstate under such adiabatic process would be

$$C_n(s) = C_n(0) \exp \left[- \int_0^s \langle \psi_n(s') | \dot{\psi}_n(s') \rangle \right] = C_n(0) e^{i\gamma_m(s)} = C_n(0) e^{i\gamma_m(s)}, \quad (3.59)$$

where $\gamma_m(s)$ is the modular Berry phase with respect to the modular parameter s .

One could change the variable s into the generalized parameter and then could write the modular Berry phase as

$$\gamma[C] = i \oint_c d\lambda(s) \langle \lambda, s | (\nabla_\lambda | \lambda, s \rangle), \quad (3.60)$$

where R here parameterizes the cyclic adiabatic process. The term $V_n = i\langle\lambda, s|(\nabla_\lambda|\lambda, s)\rangle$ is the modular Berry potential which as mentioned, we expect that considering the quantum tunneling through it would make the phase diagrams of MI, i.e, fig 5 smooth.

So when the modular time s varies in a sufficient slow manner, if the system was initially in the eigenstate $|n(\lambda(0))\rangle$, it would remain in the instantaneous eigenstate $|n(\lambda(s))\rangle$ of the modular Hamiltonian $H(\lambda(s))$ up to a phase. The complexity would change, therefore in this case, the only parameter of the state which the complexity could be proportional to would be the Berry phase. This result would be related to Chern theorem, as the Berry phase could be written in terms of the integral of Berry curvature $\omega_n(\lambda) = \nabla_\lambda \times V_n(\lambda)$, in the form $\gamma_n = \int_S dS \cdot \omega_n(\lambda)$, and this integral would be quantized in units of 2π (Chern number), pointing a connection between $e^{i\gamma_n}$ and complexity of purification (the basis complexity).

Note that in fact Chern theorem states that the integral of the Berry curvature over a closed manifold is quantized in units of 2π . We found a similar result for the complexity of purification (CoP) in [9]. Even the multipartite complexity of purification was an integer multiplet of 2π . The reason that complexity of purification, Berry curvature and Chern number are connected could be explained by how the zero modes and other normal modes and modular flow in the setup discussed in [6] would create the curvature of the bulk.

In other words, if a state change from $|\psi_n(a)\rangle$ on a path $\gamma(s)$ where $\gamma(0) = a$, which is being created by changing some parameters of the system, then we could write $|\psi(s)\rangle = e^{i\theta_n(s)} |\psi_n(\gamma(s))\rangle$. The phase could be divided into two pieces, $\theta_{n,dynamic}$ and $\theta_{n,geometric}$. Again, our conjecture is that the dynamical part of the phase change corresponds to spectrum complexity part of CoP, and the geometric part, which is related to rotation of the basis and so to Berry connection and Berry phase, would be related to basis complexity part of CoP, which one could note again the relations 3.50, 3.51 and 3.53.

The interesting point comes from the gauge transformation relation

$$|\tilde{n}(\lambda(s))\rangle = e^{-i\beta(\lambda)} |n(\lambda(s))\rangle, \quad (3.61)$$

which for an open-path gives the Berry phase $\tilde{\gamma}_n(s) = \gamma_n(s) + \beta(s) - \beta(0)$ and for a closed path would give $\beta(T) - \beta(0) = 2\pi m$ (m is an integer), which then leads to the result that the Berry phase γ_n by modulo 2π would be invariant. This fact points to another connection between the properties of complexity of purification, see the results of [9], and Berry phase.

Another connections between complexity and Berry phase could come from the results of [39] where it has been suggested there that the deformation of Euclidean path integral which prepares a state which is related to Berry phase, could provide another definition for complexity with a standard gate counting notion. So this way, the Liouville action would be related to the Euclidean analogue of the Berry phase. Since the connections between Liouville action and complexity have also already

been established in [40, 41], therefore again this would point out to our desired connections between Berry phase and complexity. This is because from the change in the measure of the path integral, one could get the exponent of the Liouville action. The procedure would be to act with the operator ρ_β

$$\rho_\beta = \exp(-\beta H), \quad (3.62)$$

on the the vacuum state. Note that H is the physical Hamiltonian operator of a $2d$ CFT on a line.

One could also write ρ_β as a circuit in the form of

$$V = \mathcal{P}\exp\left\{-\int_{t_i}^{t_f} dt \int dy [a(t, y)h(y) + ib(t, y)p(y)]\right\}. \quad (3.63)$$

So acting by this operator on the vacuum state would produce states which could be parametrized by the circuit parameter t which are different from the vacuum state but will end on the vacuum state at $t = t_f$ and the change in the measure of path integral would be the exponent of the Liouville action. This is in fact the connection between Liouville and Berry phase [42].

As we found the connections between modular Hamiltonian and complexity, the bound that has been found for modular scrambling modes could be used for complexity of purification, as the bound of 2π has been observed for both system, so we get

$$\left|\frac{d}{ds} \log F_{ij}(s)\right| \propto \text{CoP},$$

where again: $F_{ij}(s) = \left|\langle \chi_i | e^{iH_{\text{mod}}s} \delta H e^{-iH_{\text{mod}}s} | \chi_j \rangle\right|.$ (3.64)

In [9], as mentioned, we also found that in $2d$ CFTs the complexity of purification between two mixed states would be smaller than 2π where quantities such as mass m or charge q would decrease CoP. Here we make the conjecture that this bound is related to the bound for modular Hamiltonian for two regions as

$$||\Delta_\psi^{is}(R_2)\Delta_\psi^{-is}(R_1)|| \leq 1 \quad \text{for} \quad -\frac{1}{2} \leq \text{Im}[s] \leq 0. \quad (3.65)$$

We expect that dissipation (mass) and charge would decrease this bound by increasing the complex modular time s . This means that by the effects of the mass of graviton and charge, the growth rate of modular Hamiltonian would become suppressed and the internal modular time would “click” more slowly. This then affects entanglement and complexity of purification between the two mixed states.

Furthermore, recently in [35], some connections between circuit complexity and Berry phase have been discussed, as the computational cost function has been related

to Berry connection, and the Berry phase could be written in terms of Virasoro circuit complexity. For a general path, this relation could be written as

$$\mathcal{B}_{h,c}[g](\tau) = -\mathcal{C}_{h,c}[g](\tau) - i \log \langle h | \hat{\mathcal{U}}[(g^{-1}(0), 0) \cdot (g(\tau), 0)] | h \rangle. \quad (3.66)$$

In fact, there, the computational cost function has been related to the Berry connection in the unitary representation of the Virasoro group. This can be extended to complexity of purification and a corresponding Berry connection for mixed states could similarly be proposed. One could also find the connection between Berry phase and the group representation of other field theories, such as Kac-Moody algebra for the case of warped CFTs as in [41, 43].

These links between the geometric phase and complexity could further be understood intuitively as follows. Note, for instance, when an electron is spiraling along a wormhole passing through one side of a thermofield double state to the other side, the geometric phase that these electron would pick would be related to the size of the wormhole and therefore to the volume complexity, or the complexity difference between the two states. On the other hand Berry curvature is right away the only gauge-invariant quantity related to the geometric properties of the wavefunctions in the parameter space, and the links could then be clear.

Based on these results, one can deduce that the complexity of purification for crystals, in addition to their other electric properties, could also be written in term of Berry phase, since the Bloch theorem for crystals would indicate that their reciprocal space would be closed and also their Brillouin zone would have a topology of a 3-torus in $3d$ which would make the integration of Berry connection over a closed loop, and therefore all the criteria would be satisfied.

In addition, using the Berry phase, and similar to the Bohr-Sommerfeld quantization condition, complexity and specifically those notions of it in quantum field theory, could also be quantized. We could then have the relation

$$\hbar \oint ds \cdot k - e \oint ds \cdot V + \hbar \gamma = 2\pi \hbar (n + 1/2), \quad (3.67)$$

where again, here γ is the geometric phase which the electron would pick up along the closed loop of the cyclotron orbit and V is the Berry potential. For free electrons, we get $\gamma = 0$, while for the electrons in graphene it would be $\gamma = \pi$. In terms of the energy level, these values are actually related to $\alpha = 1/2$ for free electrons in the vacuum with the relation $E = (n + \alpha)\hbar\omega_c$, or $\alpha = 0$ for electrons in graphene with the relation for the energy levels as $E = \nu\sqrt{2(n + \alpha)eB\hbar}$.

Then, one could note that the Modular Berry curvature could be written as the sum over all the eigenstates as

$$\omega_{n,\mu\nu}(\lambda(s)) = i \sum_{n' \neq n} \frac{\langle n | (\partial H / \partial \lambda_\mu) | n' \rangle \langle n' | (\partial H / \partial \lambda_\nu) | n \rangle - (\nu \leftrightarrow \mu)}{(\epsilon_n - \epsilon_{n'})}. \quad (3.68)$$

For a general background which could be mixed as well, considering “all” the eigenvalues with the right degeneracies would be essential for reconstruction of bulk geometry, specially for the *mixed states*, similar to the case when we need to reconstruct any function using Fourier expansions. So one would expect instead of the definition of *index* just based on the number of zero-modes, which would be invariant under all continuous transformations, for the case of mixed states and purification, one should add all the modes to define the index which subsequently could be used for bulk reconstruction and defining EoP and Cop. For the case of our symmetric setup of figure 8, however one could just “add” those two terms in eq. 3.68, and then divide the result by two, in order to find a new quantity which contains all the normal-modes and would be more suitable enough for reconstructing the wedge cross sections of mixed states.

Also, in QCD and in heterotic string theory, the index there is the number of generations minus the number of antigerations of leptons and quarks. So, for mixed setups, to consider the effects of all EPR pairs, one actually needs to make the sum over all the eigenstates in 3.68, and then the result divided by two would be proportional to complexity of purification in [9]. Note also that using the “Atiyah-Singer index theorem”, one could specify exactly the connections between fermionic zero modes, the topology of spacetime with various genus and the anomalies.

From the parameters of the CFT one could get further information too. For instance, the interconnections between EoP and CoP and mass of graviton, m has been shown in figures, 4, 5, 6, and 7. One could see that the mass, similar to charge, would decrease both EoP and CoP. This could imply that in a gravity background when the graviton is massive, the modular Berry connection, Berry curvature and Berry phase for the massive case would be smaller than the massless case. This could also be explained by the fact that in such systems, when varying the Hamiltonian $H(\lambda(t))$, the charge or mass could decrease the rate of the process.

Comparing the diagrams of EoP versus CoP, one could deduce that modular Berry connection is more related to CoP rather than EoP, as CoP probes more space of the bulk. That is in fact why at $d = 2$, $q = 0$ and $m = 0$, CoP is very close to π but this is not the case for EoP.

By increasing the charge q , for the case of three-dimensional bulk metric, CoP decreases from π to a lower value. This could indicate that modular Berry connection could also create a potential wall which its height decreases by increasing the charge of the system. This observation has also been confirmed by studying complexity growth rate in charged black holes, [44, 45]. So charge would also decrease the modular Berry curvature.

Additionally, using the idea of [6], which considers modular Berry connection as a sewing kit for the entanglement wedge, and also the idea of quantum error connections [2, 3, 46] and the conditions for having a well defined spacetime [47], one could see that the patches of space which contains same sign charges would become

correlated. This is also true for the backgrounds where the graviton is massive, as the dissipations again would make the patches less correlated and would lower the modular Berry connections compared to the scenarios with the massless gravitons.

Moreover, note that the zero-modes could tell how the object moves in space, or superspace in the case of fermions. In the case of instantons, its zero modes would determine how the size or shape would change and this is exactly related to the holographic complexity.

For our setup which consists of mixed states of two strips, we definitely have lots of degeneracies. The Berry transformations, acting by automorphisms of energy eigenspace, can rotate these degenerate eigenstates into one another [8, 48]. The charge or mass term could then add additional terms to the initial gauge due to zero modes and therefore increase or decrease the holonomy and as the result the Berry curvature.

In fact, any conserved charge would produce new sets of modular zero-modes [6] and then these modes holographically would be mapped to the edge modes of the dual bulk gauge fields. Then, the changes in the modular Berry curvature, would change the local field strengths of the gauge fields along the HRRT surface, as we have also observed in our previous works for the case of charged or massive BTZ in [9, 49].

So as we study the change of EoP and CoP when a gauge is on, we also study how these conserved charges would change the modular zero-modes along HRRT surfaces or even the minimal wedge cross section Γ of EoP and we could then study all those effects on the correlations, modular curvature and computations through complexity and CoP. In fact, the gravitational edge modes and soft modes should specifically be studied along the minimal wedge cross section in order to understand their effects on the correlations of *mixed states*.

Also, if one considers the case of instantons in gauge theories, one needs to add additional terms to the gauge fields and build new operators which then it would have new sets of zero-modes and normal-modes. Specially, one needs to note that in the region where the instantons locate, the zero modes will be nonzero and nontrivial. So the instantons will induce multi-product interactions which as the result would play a role in changing the holonomy of bulk space time, and as we observed in [9], the entanglement of purification and complexity of purification.

As a side note, one could define a quantity using the ratio $\frac{N}{M}$ where N comes from $(|\psi\rangle_{AB} \langle\psi|)^{\otimes N}$ and M is for one of the regions A or B (for the symmetric case) as $(|\psi\rangle_A \langle\psi|)^{\otimes M}$, which could then be employed to define some new quantity for CoP similar to using LOCC. Note that in [50], the minimal area in Euclidean time dependent case has been discussed, which as they dubbed corresponds to pseudo entanglement and pseudo complexity. So, in addition to complexity of purification (CoP), other quantities such as, pseudo entanglement and pseudo complexity, or quantities such complexity of randomness which is also called unitary t-design, could also be

related to modular chaos and modular scrambling modes, and bulk reconstruction through it could be discussed.

In [22], the modular Berry transport which is being generated by two operators G_{\pm} , and the modular Berry scrambling modes, have been introduced, which could be written as

$$e^{-iH_{\text{mod}}}\delta H_{\text{mod}}e^{iH_{\text{mod}}s} \sim e^{\lambda s}G_+. \quad (3.69)$$

If similar to [22], we consider the Hermitian operator which encodes the “stripped” matrix elements of $\delta H_{\text{mod}}(s)$ at large s , then one could see that the dissipation would suppress these “stripped” matrix elements G_+ , as it would also suppress CoP. The relation $[H_{\text{mod}}, G_+] \approx e^{\lambda s}G_+$, however, would still work for the mixed systems.

In our setup, the holonomy for the space of RT surfaces for this specific case which has a gradient, see figure 8, could then be calculated. This holonomy would depend on the geometric component of the modular Berry curvature [6]. The modular Hamiltonian of an interval in the vacuum of CFT₂ with the endpoints (x_L^+, x_L^-) and (x_R^+, x_R^-) could be written as

$$H_{\text{mod}} = K + \bar{K}, \quad (3.70)$$

where $K = \pi i(L_1 - L_{-1}) = -2\pi i \sin x^+ \partial_+$, and $\bar{K} = \pi i(\bar{L}_1 - \bar{L}_{-1}) = -2\pi i \sin x^- \partial_-$.

With an infinitesimal Virasoro excitation, the modular Hamiltonian would be perturbed with the element of $Y + \bar{Y}$, which Y has the form $Y = \int dx^+ f(x^+) T_{++}(x^+)$, and similarly for \bar{Y} . When considering the massive case with m being the mass of graviton, and charged case, where q is the charge on each boundary, we expect that this would be modified similar to the higher spin case as

$$Y_{\lambda} = \int dx^+ (1 - \cos x^+)^{\frac{1+f(m)+g(q)}{2}} (1 + \cos x^+)^{\frac{1-f(m)-g(q)}{2}} T_{++}(x^+). \quad (3.71)$$

It might worth to mention here that, in our setup, we also could observe and study the size-winding, specially at low temperatures [51] which specially happens near the scrambling times. The connections between the size winding and modular Hamiltonian and modular chaos could be modeled using the time-evolved operator written in the Pauli basis in the following form

$$O(t)\rho_{\beta}^{1/2} = e^{-iHt} O e^{iHt + \frac{\beta}{2}H} = \sum_P c_P P. \quad (3.72)$$

When any two points in the strip become close enough to each other, i.e, their distance becomes smaller than D_c , the ER bridge forms between them. For this to happen, there would be some energy needed which will be taken from the vacuum energy. One could then find the expression for the modular Hamiltonian for the case of free massless fermion in $d = 2$, where as found in [52], the local term would

be proportional to energy density and the non-local part would have a quadratic expression in terms of the fermion field.

In the next sections, we discuss the specific form of modular Hamiltonian in special cases in more details.

3.3 Modular Hamiltonian, connected vs. disconnected regions

One might wonder what would be the modular Hamiltonian for connected regions versus the disconnected regions. The modular Hamiltonians for Euclidean path integral states have been studied recently in [53], and the exact formulation derived there, could point out to some analytical expressions for these two cases. In [4], the entanglement wedge reconstruction from the modular flow point of view has been discussed. They have discussed that such reconstruction could be done by integrating the modular flow against a kernel. The main assumptions in their work is based on the free field setup.

First, note that the modular Hamiltonian and modular flow for the two disconnected regions would have a stable structure. When one of two regions move toward the other one, if they are close enough but still the distance be bigger than D_c , the modular flow would oscillate and the scrambling modes of the components of modular Hamiltonian still have an upper bound of 2π . When some parts of the two regions get closer to each other than D_c , the modular flow of one region would “flow” toward the other one to form a narrow bridge connecting the two regions. At this stage of phase transition from the disconnected entanglement wedge to the partially connected case, the speed of formation for this connection and the rate of change of the components of modular Hamiltonian would be greater than 2π .

To get further intuition of the correlations behavior and modular flow in our setup, first we could imagine that both regions just be the half space and in the beginning they are far away. The subregion in the left, could then to be considered as the sources λ_i for the local operators O_i which are distributed along the half-space, left strip, and they excite the modular Hamiltonian and change the modular flow of the subregion in the right half, as shown in figure 9. As found in [53], the operators could only be the function of Lorentzian time then.

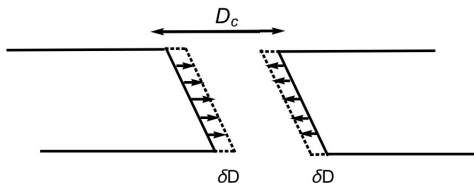


Figure 9. Perturbing the modular Hamiltonian and modular flow by bringing the two strips closer to each other infinitesimally and slowly.

If we assume that the two regions would actually move very slowly toward each other as in figure 9, we could use the results from the shape deformation section of [53] to get an intuition of how modular Hamiltonian and modular flow would change.

In the perturbation regime, the expression found for the modular Hamiltonian is

$$K_\lambda = c_\lambda + K + \sum_{n=1}^{\infty} \frac{1}{n!} \delta^n K, \quad (3.73)$$

$$\delta^n K = n! \frac{(-i)^{n-1}}{(2\pi)^{n-1}} \int d\mu_n \int_{-\infty}^{\infty} ds_1 \dots \int_{-\infty}^{\infty} ds_n f_{(n)}(s_1 + i\tau_1, \dots, s_n + i\tau_n) O(s_1, Y_1) \dots O(s_n, Y_n), \quad (3.74)$$

where K is the vacuum modular Hamiltonian, Y is the spatial coordinate on the half-space subregion, c is constant and τ is the angular coordinate around the entanglement cut which parameterizes the vacuum modular flow. Also,

$$d\mu_n = \prod_{i=1}^n d\tau_i d^{d-1} Y_i \lambda(\tau_i, Y_i), \quad (3.75)$$

which contains n powers of the source λ .

The function in the modular flowed operator relation is

$$f_{(n)}(s_1, \dots, s_n) = \frac{1}{2^{n+1}} \frac{1}{\sinh(\frac{s_1}{2}) \sinh(\frac{s_2 - s_1}{2}) \dots \sinh(\frac{s_n - s_{n-1}}{2}) \sinh(\frac{s_n}{2})}. \quad (3.76)$$

Using the above relation, the difference between the connected versus disconnected case could be studied. In fact, one could see that the factor affecting the modular Hamiltonian during the phase transition would be the singularities in the function $f_{(n)}$ which make $\delta^n K$ discontinuous.

As another observation, note that the dissipation parameter m and charge q would increase the boost times or Rindler times s_i and also the Euclidean angular or modular times τ_i and therefore they would decrease the function $f_{(n)}$ and therefore the smearing function $F_n^{(\lambda)}$ and so m and q would actually suppress the excitation terms in the modular Hamiltonian as we would have expected.

For this configuration, the operators could also be replaced as

$$O(s_i) \rightarrow a(-e^{s_i} T_{++} + e^{-s_i} T_{+-}) e^{s_i + i\tau_i} (+\delta D) + a(-e^{-s_i} T_{--} - e^{-s_i} T_{+-}) e^{-s_i - i\tau_i} (-\delta D). \quad (3.77)$$

We could assume that our deformation is null, so for the null deformations, the modular Hamiltonian could be written as

$$K = 2\pi \int d^{d-2} \vec{x} \int_{\delta \vec{D}}^{\infty} dx^+ (x^+ - \delta \vec{D}) T_{++}(x^+, 0, \vec{x}) + c_V. \quad (3.78)$$

As for the question of what would happen to modular Hamiltonian and modular flow during the phase transition from the disconnected phase to connected bulk region, one could note that when the entanglement wedge becomes connected and the states become mixed, the non-area or non-local part of modular Hamiltonian would get mixed as well and the non-local part would be similar. As this non-local part of modular Hamiltonian would mix with each other it produces a bigger holonomy in the bulk.

Note that the first order correction of modular Hamiltonian would be

$$\delta^1 K = -2\pi \int d^{d-2} \vec{x} \int_0^\infty dx^+ V^+(\vec{x}) T_{++}(x^+, \vec{x}) - 2\pi \int d^{d-2} \vec{x} \int_0^{-\infty} dx^- V^-(\vec{x}) T_{--}(x^-, \vec{x}). \quad (3.79)$$

The derivative of this relation, would be related to the Berry phase and therefore to the complexity of purification.

When the eigenstate of the initial Hamiltonian changes from $|E\rangle = |E(\lambda(0))\rangle$ to

$$\exp(-i \int_0^T E(\lambda(t')) dt') \times \exp(i \oint \Gamma_\lambda d\lambda) |E\rangle, \quad (3.80)$$

where $\Gamma_\lambda = i \langle E(\lambda) | d/d\lambda | E(\lambda) \rangle,$

then the mass and charge would decrease both Γ_λ , which is the Berry connection, and the second phase of the above relation of the closed integral, which is the Berry phase. This could simply be explained by the fact that when varying the system adiabatically, if one has a charged system or when the graviton has a small mass, the gradient $d/d\lambda |E(\lambda)\rangle$ would be smaller.

Additionally, the massive graviton states could be modeled as excited state. In [54], the perturbative techniques for studying the modular flows of general excited states have been developed which could also be used for studying modular flow for dissipative systems which are dual to states with the small graviton mass.

Note that as mentioned in [8], the second factor of 3.3, the closed integral expression, would indeed arise from the “precession” of the instantaneous Hamiltonian eigenbasis. So when the graviton is considered to be massive or when we have a (same sign) charged background, this precession would be smaller which leads to a smaller Berry phase.

Now we turn to other mathematical tools for bulk reconstructions, such as Connes cocycle flows, OPE blocks and Uhlmann holonomy.

3.4 The effects of dissipation and charge on CC flow and kink transform

At the cut between two CFTs, a stress tensor shock by the Connes cocycle (CC) flow could appear where we would like to study in this section. The boundary CC flow or one-sided modular flow is actually dual to the bulk kink transform as shown in [55]. In the bulk there is actually a Weyl tensor shock.

The unitary cocycle relation could be written as

$$U_{\psi_2\psi_1}(s)\Delta_{\psi_1}^{is}O\Delta_{\psi_1}^{-is}U_{\psi_2\psi_1}^\dagger(s) = \Delta_{\psi_2}^{is}O\Delta_{\psi_2}^{-is}, \quad \forall O \in \mathcal{A}, \quad (3.81)$$

where for the massive case, this relation would in fact be approximate. The operator $\Delta_\psi = S_\psi^\dagger S_\psi$ is a positive operator called *modular operator* and S_Ψ is an anti-linear operator acting as

$$S_\Psi O |\Psi\rangle = O^\dagger |\Psi\rangle, \quad \forall O \in \mathcal{A}(R). \quad (3.82)$$

We expect that the unitary cocycle flow would also act as a quantum recovery channel and actually these two would be related through the Hadamard three-line theorem and complex interpolation. The applicability of using Petz map for recovering quantum information would be dual to remaining in the code subspace which also related to structure of quantum Markov chain, meaning being close enough to the code subspace, we could model the local correlations similar to the quantum Markov chains.

The connections between cocycle flow and quantum recovery channel could also be observed from the result of [56], where they found that the commutator

$$\begin{aligned} C_{\text{see}} &= \langle \psi | [\tilde{O}, \Delta_{\psi;\mathcal{A}}^{-is} \phi \Delta_{\psi;\mathcal{A}}^{is}] | \psi \rangle = \\ &\langle \psi | \Delta_{\psi;\mathcal{A}}^{is} \Delta_{\Omega;\mathcal{A}}^{-is} O \Delta_{\Omega;\mathcal{A}}^{is} \Delta_{\psi;\mathcal{A}}^{-is} | \psi \rangle, \end{aligned} \quad (3.83)$$

could detect the information beyond the causal wedge.

All of these cocycle flows would actually be added together and then build up the final modular flow. The quantum recovery channels could also be modeled using them as well. Therefore, we expect that the quantum recovery channels which are needed in the bulk reconstruction procedure, could also bring operators out from entanglement islands similar to the work of [57].

From the symmetries of modular scrambling modes, $\delta H_{\text{mod}} |\psi\rangle = 0$, which would lead to $G_\pm \psi \approx 0$, and their duals which are proposed to be the local Poincare symmetry groups of the bulk, we can conclude that the change in modular Hamiltonian and the application of cocycle flow, is dual to the change in the curvature of the bulk. The bigger the change of modular flow, the deeper the quantum circuit would be with a bigger complexity, and with more quantum recovery channels which then would lead to a bigger curvature in the bulk. Therefore, black holes are the systems with the ability to change the modular flow fastest, which then means more cocycle flows, and deeper quantum circuits, with the highest complexity. It worths to mention here that actually, by passing more ‘‘modular time’’, s , extracting the geometric quantities would become more precise and close to the RT surface, one could zoom-in further.

It is also interesting to study the effects of dissipation and charge on reconstructing the bulk through the mixed correlations, using the boundary connes cocyle flow

of $|\psi\rangle$ as our toy model which actually would generate a family of states $|\psi_s\rangle$ as

$$|\psi_s\rangle = (\Delta'_\Omega)^{is} (\Delta'_{\Omega|\psi})^{-is} |\psi\rangle, \quad (3.84)$$

where the relative modular operator is $\Delta_{\psi|\Omega} \equiv S_{\psi|\Omega}^\dagger S_{\psi|\Omega}$. Note that the modular Hamiltonian here could be written as $\widehat{K}_{V_0} = -\log \Delta_{\Omega; A_{V_0}}$.

For the arbitrary cuts of Rindler horizon one would have the relation

$$\Delta \langle K'_{V_0} \rangle = -2\pi \int dy \int_{-\infty}^{V_0} dv [v - V_0(y)] \langle T_{vv} \rangle_\psi. \quad (3.85)$$

From this relation, the effect of dissipation and charge on modular Hamiltonian, through the effects on “energy momentum tensor” components could be observed, and then their effects on CC flow could be found out. One could see that both of these parameters would *suppress* the CC flow.

In fact, we could write the following relation for the CC flow of stress tensor as

$$\langle \psi_s | T_{vv} | \psi_s \rangle |_{v < V_0} = e^{-4\pi s} \langle \psi | T_{vv} (V_0 + e^{-2\pi s} (v - V_0)) | \psi \rangle |_{v < V_0}. \quad (3.86)$$

So, one could see here too that the dissipation and same sign charge would actually increase s and therefore this CC flow of energy-momentum would be suppressed as well.

Also, the shape derivatives of modular Hamiltonian which could be written as

$$\left. \frac{\delta \langle K'_V \rangle_\psi}{\delta V} \right|_{V_0} = 2\pi \int_{-\infty}^{V_0} dv \langle T_{vv} \rangle_\psi, \quad (3.87)$$

would be suppressed as well since the components of energy momentum tensor would become smaller due to the effects of dissipation and same-sign charges.

Then, note that the dual of CC flow which is the bulk “kink transform” [55] could be written in the form of

$$(K_\Sigma)_{ab} \rightarrow (K_{\Sigma_s})_{ab} = (K_\Sigma)_{ab} - \sinh(2\pi s) x_a x_b \delta(\mathcal{R}). \quad (3.88)$$

These transformations then, by combinations of modular operators could generate some sequences of global states ψ_s . These then could point out to its relation to complexity of building states using the intuitions from [58]. Actually the rapidity of $2\pi s$ which is being formed by the relative boost which glues entanglement wedges A and its complement A' would be connected to the value we found for the complexity of purification which was 2π in $2d$.

The effects of the dissipation parameters or m in the holographic bulk spacetime and also the same-sign charge could be also be seen using the above relation 3.88. Once again one could see, through their effects on “ s ”, these two parameters would actually suppress the *kink transform*.

3.5 Entanglement wedge cross section from OPE blocks

In this section, we comment on the “geodesic operator/OPE block dictionary” to understand the complexity of purification, mixed state correlations of two strips, the bit thread and wedge reconstruction better.

On the boundary CFT, the zero modes of $H_{mod}(\lambda)$ would make the OPE blocks, which come from two spacelike separated local operators in the form of

$$\mathcal{O}_L(x_L)\mathcal{O}_R(x_R) = \sum_{\Delta} |x_R - x_L|^{-\Delta_L - \Delta_R} c_{LRi} |x_R - x_L|^{\Delta} (\mathcal{O}_{\Delta} + \text{descendants}), \quad (3.89)$$

where the OPE blocks are actually the second part as

$$\text{OPE Block } B_{\Delta}^{\kappa}(\lambda) \rightarrow |x_R - x_L|^{\Delta} (\mathcal{O}_{\Delta} + \text{descendants}). \quad (3.90)$$

For a finite transformation s_0 , the OPE blocks transform as

$$B_{\Delta}^{\kappa}(\lambda) \rightarrow e^{s_0 \kappa} B_{\Delta}^{\kappa}(\lambda), \quad (3.91)$$

which is a change of normalization.

The holographic dual of a scalar OPE block is a bulk operator in the form [8, 11, 59]

$$B_{\Delta}^{\kappa}(\lambda) = N \int_{[\lambda]} ds \phi_{\Delta}(s) e^{-\kappa s}, \quad (3.92)$$

where here s is the proper length parameter along the bulk geodesic $[\lambda]$ (in the units of L_{AdS}) and ϕ_{Δ} is the bulk operator dual to \mathcal{O}_{Δ} .

Note that any product scalar of two operators $O_1(x_1)$ and $O_2(x_2)$ could be expanded in terms of OPE block which are some primary operators that are being smeared in a causal diamond \diamond_{12} and so it could be written as [11],

$$\mathcal{B}_k(x_1, x_2) = \frac{\Gamma(2h_k)\Gamma(2\bar{h}_k)}{\Gamma(h_k)^2\Gamma(\bar{h}_k)^2} \int_{\diamond_{12}} dw d\bar{w} \left(\frac{(w - z_1)(z_2 - w)}{z_2 - z_1} \right)^{h_k - 1} \left(\frac{(\bar{w} - \bar{z}_1)(\bar{z}_2 - \bar{w})}{\bar{z}_2 - \bar{z}_1} \right)^{\bar{h}_k - 1}, \quad (3.93)$$

where the left and right moving conformal weights are $h_k = \frac{1}{2}(\Delta_k + \ell_k)$ and $\bar{h}_k = \frac{1}{2}(\Delta_k - \ell_k)$ and Δ_k and ℓ_k are the scaling dimension and spin of the quasiprimary operators \mathcal{O}_k . The parameter which is being changed by the mass of graviton m or charge of the fields q would be h_k which changes the nature of OPE blocks in the bulk reconstructions.

The complexity of purification for the mixed states would then be related to the number of quasiprimary operators, \mathcal{O}_k , which are needed to produce the \diamond_{12} with enough, desired precision. The sewing of patches of various causal diamonds

◇ would create the bulk entanglement wedge for us. So the similarities between the summation of causal diamonds and other bulk reconstruction methods such as recovery channels and modular flows could be seen here.

Note that in the bulk, the dual of the boundary causal diamond would be a geodesic operator. Then, there is the equality of OPE blocks and the X-Ray/ Radon transforms, which even in higher dimensions, and for time-like separated pairs, the OPE blocks could be considered as surface Witten diagram which could be written as

$$g_k(u, v) = \frac{1}{(c_\Delta^s)^2} \int_{\sigma_{12}} d^{d-2}z \int_{\sigma_{34}} d^{d-2}z' G_{bb}(z, z'; m_k). \quad (3.94)$$

Here, x_1, x_2 and x_3, x_4 are the endpoints of the two intervals. This non-local quantity, could be considered similar to our notion of volume interval (VI) [9] as a measure of complexity of purification for mixed states.

We expect that the integral of bulk fields along the minimal wedge “cross section”, and therefore the OPE blocks would be proportional to the entanglement of purification as well, since we have

$$c_\Delta \mathcal{B}_k(x_1, x_2) = \tilde{\phi}_k(\gamma_{12}) = \int_\Gamma ds \phi(z), \quad (3.95)$$

where $c_\Delta = \Gamma(\frac{\Delta}{2})^2/2\Gamma(\Delta)$ is just a constant.

The relationship between the space of causal diamond which is a coset space and is being defined as

$$\mathcal{K} = \frac{SO(2, 2)}{SO(1, 1) \times \overline{SO(1, 1)}} = \frac{SO(2, 1)}{SO(1, 1)} \times \frac{\overline{SO(2, 1)}}{\overline{SO(1, 1)}}, \quad (3.96)$$

and the minimal entanglement wedge cross section and the flow of modular zero modes $B_i(\lambda)$ and Berry flow could then be considered. We conjecture that the tips of all causal diamonds have a decreasing flow from the point m to m' and also as the OPE block transform as $\mathcal{B}_\Delta^\kappa(\lambda) \rightarrow e^{s_0\kappa} \mathcal{B}_\Delta^\kappa(\lambda)$, the parameter s_0 becomes smaller when moving from the point m to the point m' .

Another point worths to mention, is that a $2d$ causal diamond would be stabilized by an $SO(1, 1) \times \overline{SO(1, 1)}$ group. The anti-symmetric combination of these two $SO(1, 1)$ which is being called $P_D(\lambda)$ in [8], satisfy the relation

$$[P_D, \mathcal{O}_L \mathcal{O}_R] = i\kappa \mathcal{O}_L \mathcal{O}_R, \quad (3.97)$$

where $\kappa = \Delta_R - \Delta_L$. Note that the dissipation parameter and also the same sign charge would suppress κ as they could suppress the dilatation and transformation generated by P_D .

A related point is that, considering the light-cone cuts [60, 61] in the bulk of two points of p and q , i.e, $C^-(p)$ and $C^-(q)$ would be intersected at a single point X and

they would be regular at that point, then these two points p and q are null-separated. This point would also be very important in reconstructing the mixed states. From the data of the boundary mixed CFTs, then one could determine the cut in the bulk, as whether it would be a connected one if its radial coordinate is above the point m' , i.e, $z_{m'} < z < z_m$, or disconnected, if $z < z_m$, or non-existent if $z > z_{m'}$.

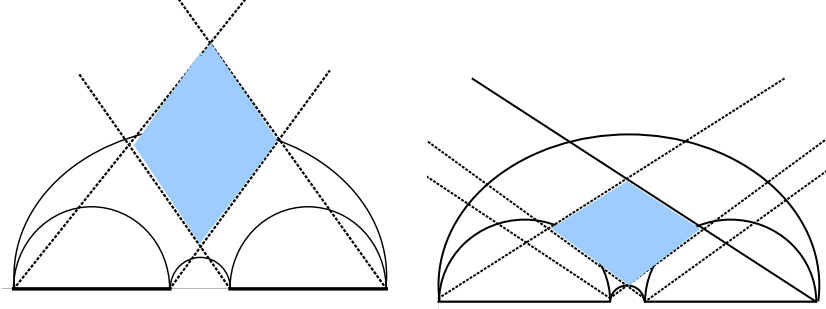


Figure 10. Various conditions for the shape of mutual diamond between two subregions. It could either be completely inside the entanglement wedge or partially inside it, depending the size of strips and the distance between them.

The connection between causal wedge and mutual information could also point out the way to reconstruct the dual of mixed states. In fact, in a recent paper [62], the connections between entanglement wedge reconstruction and mutual information through the holographic scattering has been discussed. Using the null vectors, the light cone cuts could be constructed for the boundary strips which would lead to various forms of the “*mixed diamond*” between the two states as shown in figure 10. Using the OPE block structure the position of mutual diamond inside the entanglement wedge could be studied. We leave the detailed numerical calculations of these studies to future works.

3.6 Uhlmann holonomy for mixed states

In this section, we turn to another tool in studying the wedge reconstruction. In [12], it has been proposed that the dual of the symplectic form of the bulk fields in any entanglement wedge would be the curvature of the Uhlmann phase. In another word, for the mixed states, the symplectic form of the bulk fields would be dual to the Uhlmann holonomy of the parallel transport of purifications of density matrices of the boundary which is the maximization of the transition probabilities.

The symplectic form of the fields in the bulk is in the form of

$$\Omega = \int_{\Sigma} \omega, \quad (3.98)$$

which is the integral of

$$\omega[\phi, \delta_1\phi, \delta_2\phi] = \delta_1(\theta[\phi, \delta_2\phi]) - \delta_2(\theta[\phi, \delta_1\phi]) - \theta[\phi, [\delta_1\phi, \delta_2, \phi]], \quad (3.99)$$

and the parameters could be defined by the variation of the Lagrangian as

$$\delta L = L[\phi + \delta\phi] - L[\phi] = \delta\phi \cdot E + d\theta. \quad (3.100)$$

On the other hand, in the dual boundary theory, for two states with parallel purifications, the fidelity would be

$$|\langle\psi_2|\psi_1\rangle| = \text{tr} \left(\sqrt{\sqrt{\rho_1}\rho_2\sqrt{\rho_1}} \right), \quad (3.101)$$

and the replicated fidelity could be defined as

$$F_k = \text{tr} \left((\sqrt{\rho_1}\rho_2\sqrt{\rho_1})^k \right). \quad (3.102)$$

Considering a closed curve $C : S^1 \rightarrow \mathcal{H}$ and the sequence of n states in the form of $|\psi_1\rangle, |\psi_2\rangle, \dots, |\psi_n\rangle$, then, for the limit of $n \rightarrow \infty$ where the states $|\psi_i\rangle$ covers the curve C , one would get

$$\langle\psi_1|\psi_n\rangle\langle\psi_n|\psi_{n-1}\rangle \dots \langle\psi_3|\psi_2\rangle\langle\psi_2|\psi_1\rangle \longrightarrow \exp(i\gamma), \quad (3.103)$$

where the Berry phase (or the Uhlmann phase) is $\gamma = \oint_C a$ and a is defined as $a = i\langle\psi|d|\psi\rangle$, which is a real 1-form. The Berry connection is defined by the transformation $a \rightarrow a - df$ which is a $U(1)$ connection, and the Berry curvature which is gauge-invariant is defined as $da = id\langle\psi| \wedge d|\psi\rangle$. One question is that how much this phase (in the bulk side) would change with changing the position of the curve C with respect to the two correlated intervals that we consider. For mixed states, the Uhlmann phase along a curve C is just the same as $e^{i\gamma} = \lim_{n \rightarrow \infty} \langle\psi_1|\psi_n\rangle\langle\psi_n|\psi_{n-1}\rangle \dots \langle\psi_2|\psi_1\rangle$.

Then using holography, the boundary replicated fidelity for the case of $k = 1/2$, could be written in terms of an on-shell gravitational action where the sources are on the boundary. So, we get

$$F_k = \exp \left(kS(\lambda_1, \lambda_2) + kS(\lambda_2, \lambda_2) - S^{(k)}(\lambda_1, \lambda_2) \right), \quad k = 1/2. \quad (3.104)$$

Therefore, the bulk symplectic form and the boundary Uhlmann phase would be connected to each other holographically, using the relation 3.104.

The curvature of the integral of the abelian connection which is the Berry phase along the Uhlmann parallel path would then be the symplectic form of the entanglement wedge and consists of flux tubes between the mixed states. The relative (total)-mode frames would then be related to the modular Uhlmann connection.

In each side, the effects of dissipation or m and charge, q , on the bulk symplectic form and on boundary Uhlmann phase could then be considered. Since these two would suppress $\delta\phi$, they would then suppress δL and then the fidelity between two states and as the result the Uhlmann phase would be suppressed which again the duality is being checked this way.

In [63], the method for observing the topological Uhlmann phase with superconducting qubits for topological insulators has been reported. They used an ancillary system and some particular interferometric techniques.

The single qubit density matrix could actually be written in terms of $\theta(t)|_{t=0}^1$ as

$$\rho_\theta = (1-r)|0_\theta\rangle\langle 0_\theta| + r|1_\theta\rangle\langle 1_\theta|, \quad (3.105)$$

where r quantifies the mixedness between the two states of $|0_\theta\rangle$ and $|1_\theta\rangle$. These two states are kind of a transmon qubit introduced in [64].

The evolution of the purification of ρ_θ would then be in the following form

$$\begin{aligned} |\Psi_{\theta(t)}\rangle &= \sqrt{1-r}U_S(t)|0\rangle_S \otimes U_A(t)|0\rangle_A \\ &+ \sqrt{r}U_S(t)|1\rangle_S \otimes U_A(t)|1\rangle_A, \end{aligned} \quad (3.106)$$

where $|0\rangle = \begin{pmatrix} 1 \\ 0 \end{pmatrix}$ and $|1\rangle = \begin{pmatrix} 0 \\ 1 \end{pmatrix}$ is the basis, S stands for the system and A for the ancilla. Then, the Uhlmann parallel transport condition is satisfied when the distance between the two infinitesimally close purifications, $\| |\Psi_{\theta(t+dt)}\rangle - |\Psi_{\theta(t)}\rangle \|^2$, becomes minimum, which physically means that the accumulated phase which is the Uhlmann phase Φ_U would be completely geometrical and not dynamical. So due to the holographic duality, their interferometric technique of observing Uhlmann phase could show a way to measure the properties of the symplectic form and quantum gravity characteristics in the bulk. Therefore this method could then paint the CFT entanglement structures and bulk gravity curvature properties in more details, as we also did some few steps in [65].

These studies could then point out to some specific intrinsic properties of space time and gravity and specially topological gravity, which is independent of dynamics of the system as Berry phase and Uhlmann phase are so too. For example the connections between some differential geometric properties of bulk could further be examined by studies of Uhlmann phase. Case in point, the extremum of the Kähler potential, $\mathcal{K} = \log\langle\alpha|\alpha\rangle$, corresponds to the minimum of the entanglement wedge cross section for two mixed states. The connections between Kähler potential and Berry curvature and complexity then could be studied. The Kähler potential is actually a real-valued function, which is being denoted by f here, defined on a Kähler manifold for which the Kähler form ω could be written as $\omega = i\partial\bar{\partial}f$, where here

$$\partial = \sum \frac{\partial}{\partial z_k} dz_k, \quad \bar{\partial} = \sum \frac{\partial}{\partial \bar{z}_k} d\bar{z}_k. \quad (3.107)$$

The Berry curvature in terms of the Kähler potential could then be written as

$$\mathcal{A} = \frac{i}{2}\partial_{\alpha_i}\mathcal{K}d\alpha_i - \frac{i}{2}\partial_{\alpha_i^*}\mathcal{K}d\alpha_i^* = \frac{i}{2}(\partial - \partial^*)\mathcal{K}. \quad (3.108)$$

For the minimum entanglement wedge cross section, this Berry curvature becomes zero.

For other aspects, note that the relative modular frame along the RT surface is actually encoded in the connection on the relevant bundle. For the mixed states, the mode frames along the minimal wedge cross section Γ , would create the modular Uhlmann connection. However, the strength of this connection depends on the mutual information and therefore on the distance between the two subregions. So the gradient of the modes along Γ depends on $\frac{dI}{dD_x}|_{\Gamma}$ or $\frac{dE_W}{dD_x}|_{\Gamma}$. This pattern is actually the same pattern of the Wilson lines which is also being dictated by the pattern of entanglement of purification and mutual information among the subsystems. The form of the dressing of gauges, which is dual to the pattern of EoP, would dictate the structure of curvature in the bulk.

The pattern of the mutual information and the entanglement of purification between the two subsystems are actually being determined by the pattern of the physical Wilson lines “dressing in gauge theories”. Wilson lines could be written in the form of

$$U[x_i, x_f; C] = \mathcal{P} \exp \left(i \int_{\tau_i}^{\tau_f} d\tau \frac{dx^\mu}{d\tau} A_\mu(x(\tau)) \right) = \mathcal{P} \exp \left(i \int_{x_i}^{x_f} A \right). \quad (3.109)$$

The non-local dressing pattern of Wilson lines in the setup of mixed states could also be studied using the mirror operator $\tilde{\sigma}_B$ introduced in [66] and being used in [6] which is in the form of $\tilde{\sigma}_{B,ij} = W_{ki} \sigma_{A,kl}^* W_{jl}^{-1}$.

Moreover, as mentioned in [8], the modular Berry transformations could actually recognize the bulk operators which are localized on the Ryu-Takayanagi surfaces. So for two subregions of A and B which correspond to two mixed states, the RT surfaces which probe the entanglement wedge cross section between them as shown in the figure 8, where also the bit threads and also the bulk operators are located, would be related to the CFT modular Berry transformations. So this way the modular Berry transformation would be related to the bit thread structures as well. For the AdS and BTZ bulk backgrounds, the conformal symmetry structures would then become handy in the calculations there.

4 Correlation Measures for Mixed States and Quantum Discord

In this section, we aim to study the nature of correlations among mixed systems further. Using some new correlation measures, we also study the effects of dissipation and charge in our setup as well.

As a first step, note that the relative entropy which is a measure of distinguishability between two states which could be a reference vacuum state σ and another

state ρ is defined as

$$S(\rho|\sigma) = \text{Tr}[\rho \log \rho - \rho \log \sigma]. \quad (4.1)$$

This quantity would also have some connections with strength of correlation and therefore the purification (EoP or CoP), which we would like to study further. Note that this quantity would actually be related to the free energy difference between ρ and vacuum at temperature $\beta = 1$. If there is more correlations, the free energy that one would be able to extract, would be lower. Therefore, EoP and relative entropy would have an inverse behavior relative to each other. It means that when two states are really different from each other, making $S(\rho|\sigma)$ bigger, EoP would be smaller meaning they are less correlated.

One then can define various measures for quantum correlations. For instance, in [67], the Uhlmann fidelity was proposed for Gaussian states. The form of their quantity $N_F^{\mathcal{G},A}(\rho_{AB})$ is

$$\begin{aligned} N_F^{\mathcal{G},A}(\rho_{AB}) &= \sup_{U \in \mathcal{U}_{\rho_{AB}}} C^2(\rho_{AB}, (U \otimes I)\rho_{AB}(U^\dagger \otimes I)) \\ &= \sup_{U \in \mathcal{U}_{\rho_{AB}}} \{1 - F(\rho_{AB}, (U \otimes I)\rho_{AB}(U^\dagger \otimes I))\}, \end{aligned} \quad (4.2)$$

where as mentioned before, the Uhlmann fidelity, $F(\rho, \sigma) = (\text{Tr} \sqrt{\sqrt{\rho}\sigma\sqrt{\rho}})^2$, is a measure of closeness between the two states, and the sine metric is $C(\rho, \sigma) = \sqrt{1 - F(\rho, \sigma)}$, and also the supremum should be taken over all Gaussian unitary operators, $U \in \mathcal{U}_{\rho_{AB}}$.

After applying any Gaussian channel, Φ , we would then have $N_F^{\mathcal{G}}(I \otimes \Phi(\rho_{AB})) \leq N_F^{\mathcal{G}}(\rho_{AB})$, which means that this measure is non-increasing under any Gaussian quantum channels. For our setup of two strips of A and B , the parts which are further away from each other and therefore less correlated would have smaller $N_F^{\mathcal{G}}(I \otimes \Phi(\rho_{AB}))$ which corresponds to the regions where more quantum channels have been applied to the subsystems. We could show that the density of modular flow would also decrease there.

For the case of (1+1)-mode ‘‘symmetric squeezed thermal state (SSTS)’’ $\rho_{AB}(n, \mu)$, of [67], in their equation 4, the relations between the correlation measure $N_F^{\mathcal{G},A}$ and the two parameters denoted by n and μ have been derived. Actually, μ is the mixing parameter where $0 \leq \mu \leq 1$ and n would be the mean photon number for each part. In figure 11, we present several plots to show the relations between the correlation measure $N_F^{\mathcal{G},A}$ versus the parameters μ and n .

It could be seen that the mixing parameter μ would actually increase this correlation measure. We expect that parameters such as mass of graviton which is related to dissipation and the same sign charge which actually decreases the mixing parameter would also decrease this specific correlation measure between the mixed systems. As both entanglement of purification (EoP) and complexity of purification (CoP) are

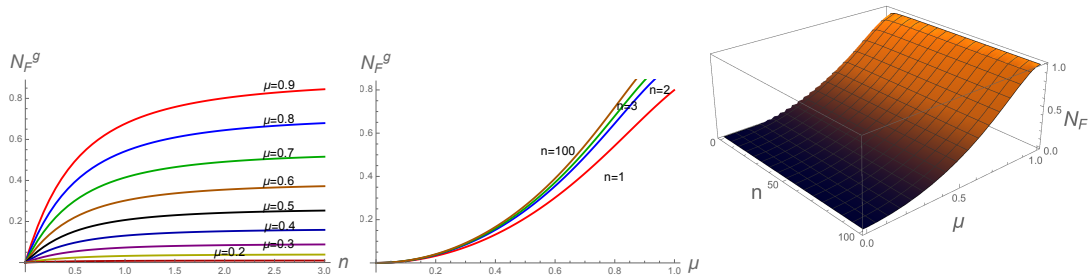


Figure 11. The relation between the correlation measure $N_F^{\mathcal{G},A}$ versus μ and n .

two other measures of correlation between mixed systems, we see that since m and q would decrease μ , therefore, these quantities also decrease EoP and CoP as well and in fact this is what we have observed in [9].

Another point comes from the definition of the channel capacity which is in the form of

$$C_E(\mathcal{N}) = \max_{\text{all } p_i, q_i} I(A : B), \quad (4.3)$$

where the maximization is over all input ensembles of the mutual information between the two systems. As the parameters such as dissipation parameter m , or the same-sign charge q of the boundary would decrease $I(A : B)$, and also the mixing parameters, we could see that they also decrease the capacity of the quantum channels. Therefore, entanglement and complexity of purification behave the same way as the quantum channel capacity under changing the parameters such as dissipation and charge, as these would decrease the mixing parameter. We would expect that decreasing the quantum channel capacity then decreases the modular flows between the two subregions.

This could also be seen from the definition of modular flow being written as

$$U_\sigma(s)\mathcal{A}_L U_\sigma^\dagger(s) = \mathcal{A}_L, \quad U_\sigma(s)\mathcal{A}_R U_\sigma^\dagger(s) = \mathcal{A}_R, \quad U_\sigma(s) \equiv \Delta_\sigma^{-is}, \quad (4.4)$$

where

$$K_\sigma^R = -\log \rho_\sigma^R, \quad K_\sigma^L = -\log \rho_\sigma^L, \quad K_\sigma^L = J_\sigma K_\sigma^R J_\sigma, \quad \Delta_\sigma = \rho_\sigma^L \otimes (\rho_\sigma^R)^{-1}. \quad (4.5)$$

Generally the dissipation makes the eigenvalues of the density matrix smaller. Also, the same sign charge suppresses the operator Δ as it decreases the entanglement between the physical modes among L and R and therefore q would suppress the modular flow.

This is also the case for the relative entropy between two states $|\Psi\rangle$ and $|\Omega\rangle$,

$$D(\rho|\sigma) = -\langle \rho | \log \Delta_{\sigma\rho} | \rho \rangle. \quad (4.6)$$

These results about the effects of m and q are also true for the difference between two modular operators, which could be seen from relations 3.34 - 3.43 of [54], as charge and dissipation increase the “distance” between the clicks of modular time and therefore decrease the terms $\frac{g_e(t_{i+1}-t_i)}{\cosh(\pi t_i)\cosh(\pi t_{i+1})}$.

Also, as $N_F^{\mathcal{G},A}$ qualitatively behaves very similar to various measures of quantum discord, we expect that these discussions also apply for them too. This could be seen from figure 12, which as one could check, the behavior is qualitatively similar to $N_F^{\mathcal{G},A}$.

Note that the Gaussian quantum discord could be written as [67]

$$D(\rho_{AB}) = S(\rho_A) - S(\rho_{AB}) + \inf_{\Pi} \int p(z)S(\rho_B(z))dz, \quad (4.7)$$

where $\Pi = \{\Pi(z)\}$ is a collection of positive operators in the form $\Pi(z) = D(z)\tau D^\dagger(z)$. Here $D(z)$ are the Weyl operators and τ is a n -mode Gaussian state. Additionally, $p(z) = \text{Tr}(\rho_{AB}\Pi(z) \otimes I)$.

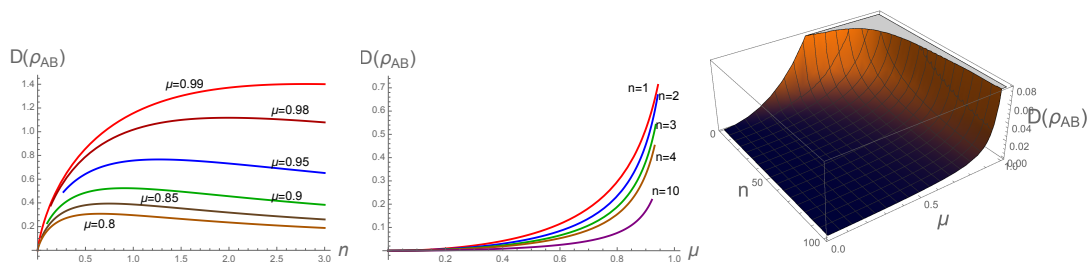


Figure 12. The behavior of the geometric quantum discord versus μ and n .

From these plots again one could see that increasing mixing parameter would increase the discord. So as quantities such as dissipation and same sign charge would decrease the mixing parameter μ , therefore they decrease the quantum discord between the two systems which then would decrease both the EoP and CoP as well. However, the behavior versus the mean photon number is opposite of the case of $N_F^{\mathcal{G},A}$.

The connection between modular Hamiltonian, Fisher information metric and this new measure could also be analyzed. Specifically the case which one has the entanglement plateau [68], i.e, when the entanglement entropies of the two regions saturate the Araki-Lieb inequality,

$$|S(A) - S(B)| \leq S(AB), \quad (4.8)$$

would be of particular interest as one could detect similar behaviors.

Also, recently in [69], for the pure states, from the Bures metric as an example of an information metric, the entanglement wedge of a two-dimensional holographic

CFT which is a time-slice of an AdS metric, has been constructed. The alternative quantity for the mixed state also has been discussed. Therefore, one could contemplate the links between modular Berry connection, Bures metric and these new measures for the bulk reconstruction procedures.

5 Modular Hamiltonian in QCD

When the system is mixed, it could be simulated using various QCD or superconducting models. Some interesting properties of these models could be seen in the connections between CFT characteristics and bulk reconstruction models. For instance, in these models, for various quantities such as Roberge-Weiss (RW) periodicity in lattice QCD or periodicity for $\mu_I/T = \theta$, or for pressure, entropy density, etc [70], always a 2π periodicity is being observed. These mixed states could then be modeled by dual quark condensations as [70]

$$\sigma^{(n)} = \int_0^{2\pi} \frac{d\phi}{2\pi} \sigma(\phi) e^{in\theta} d\phi, \quad (5.1)$$

where $\sigma(\phi)$ is the chiral condensate and the phase of the boundary condition is in the range $0 \leq \phi \leq 2\pi$. Note that this phase is related to the dimensionless imaginary chemical potential as $\phi = \theta + \pi$.

One observation we made was that this imaginary property of QCD potential is in fact related to the imaginary behavior of complexity of purification and both behave with a periodicity of 2π and also the Roberge-Weiss (RW) periodicity. Some notion similar to the imaginary chemical potentials could also be defined for modular flows and modular Hamiltonians.

The mechanism of getting information from the confining phase, using modular flow, would also be similar to what has been examined in [57]. In the exact moment of transitions between confining and deconfining phases, the quark-gluon plasma phase could be considered as the island, and the de-confined surrounding gas could be considered as the heath bath. So the mechanisms of extracting information from the island to the bath using the modular flow could give information about the interaction of information and modular flow in QCD as well. Also, the quasi-localness of modular Hamiltonian would have a significant role in the behavior of QCD which we would like to study here.

The non-local piece of modular Hamiltonian for free fermions has been found as

$$H_0 = -2\pi i \sum_{l=1}^n \frac{1}{x-y} \left(\frac{dz}{dy} \right)^{-1} \delta(y - x_l(z(x)), \quad x_l(z(x)) \neq x, \quad (5.2)$$

which indeed agrees with our expectations from the behavior of entanglement structures for mixed states and intuitions from the bit threads construction in our setup.

Using relations of [57, 71] for free fermions in $2d$, the plots of various trajectories of left-moving operators, during the flow, have been shown in figure. 13. The two intervals are actually $[a_1, b_1]$ and $[a_2, b_2]$. Note that many aspects of QCD could also be modeled by many-fermion systems.

One interesting observation here is that the modular flowed operators and the correlations among them in fact could frame the structures of entanglement and complexity of purification. This could be seen from the relations 4.2, 4.5 and 4.9 of [53] and 19, 21, and 57, 58 of [17]. For our case, we should consider various operators at the same modular times but distributed along the minimal wedge cross section Γ , where the distribution function of the source have the form

$$g(s, s + i\tau') = -\frac{1}{2} \frac{\sinh(\frac{s}{2})}{\sinh(\frac{s+i\tau'}{2}) \sinh(\frac{i\tau'}{2})}. \quad (5.3)$$

If we consider two operators in the two regions, they are time-like separated and we could have still the following relations for the modular time as

$$s'_{*,\pm} = s + \log(\alpha \pm \sqrt{\alpha^2 - 1}), \quad \alpha = \frac{x_1^2 + z_1^2}{x_1 z_1}. \quad (5.4)$$

Exactly on the minimal wedge cross section, the modular time would have the same structure as those approaching the entanglement cut, $x^1 \rightarrow 0$, so it would be like a boost operator but multiplied by a factor of two.

For the two regions in pure AdS₃, this then, would lead to the following relation for the entanglement of purification as

$$E_w(\rho_{AB}) = \frac{c}{6} \log(1 + 2z + 2\sqrt{z(z+1)}), \quad \text{where } z = \frac{(a_2 - a_1)(b_2 - b_1)}{(b_1 - a_2)(b_2 - a_1)}, \quad (5.5)$$

where the two regions are $A = [a_1, a_2]$ and $B = [b_1, b_2]$ where $a_1 < a_2 < b_1 < b_2$.

Note that the entanglement cut and E_W would both be approached when we get $x^1 \rightarrow 0$ and $\alpha \rightarrow \infty$. Also, modular flow would act as a local boost exactly on the minimal wedge cross section line, Γ .

The fact that, along the imaginary axis, the modular cuts would be repeated with period of 2π , would be again related to the fact that in $2d$, the CoP would be 2π as well. This would also be related to the periodicity of QCD potential which is proportional to 2π , as we will explain further in the next part.

For more examinations, our specific setup would be two intervals of $[-1, -0.1] \cup [0.1, 1]$. This simple example could act as a toy model to further understand the behaviors of modular flow, and the mechanisms of extraction of information from the islands, in the mixed and more complicated setups.

When the intervals are closer to each other, or when their widths are bigger, the modular flows are stronger. The system with a stronger flow is shown in the down-left part of figure 13 and the weaker one is shown in the top-right. As for the QCD,

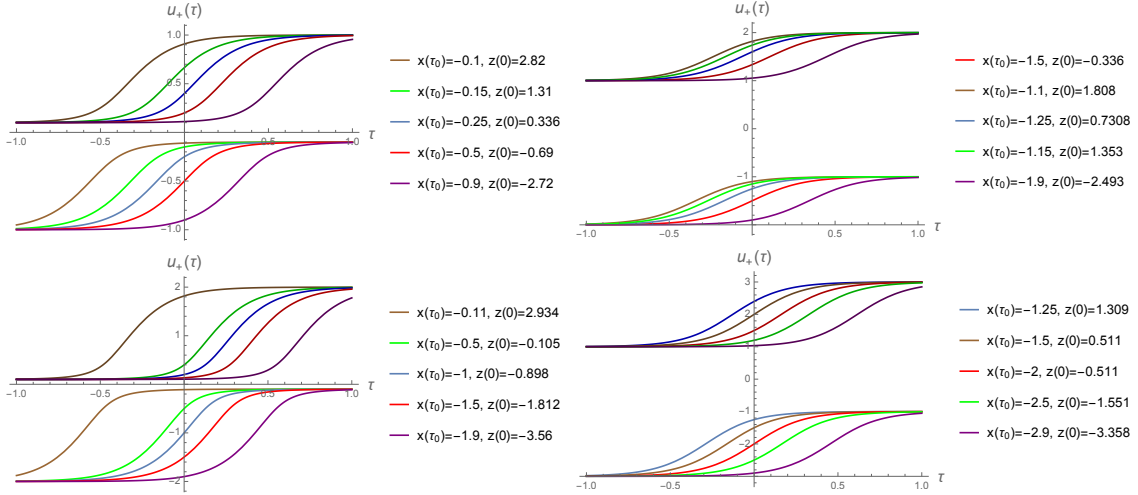


Figure 13. Various trajectories of left-moving operators during the flow, with different initial values for $x(\tau = 0)$ and $z(0)$ for the setup of two intervals of $[-1, -0.1] \cup [0.1, 1]$ in top left part, $[-2, -1] \cup [1, 2]$ in the top right part, $[-2, -0.1] \cup [0.1, 2]$ in the down left part and $[-3, -1] \cup [1, 3]$ in the down right part.

these observations could denote that the parameters which make the confined phase more compressed, such as pressure, then make pulling information out of islands more difficult.

The relation for the angle $\theta(\tau)$ which determines how the fermion operator would flow under modular Hamiltonian as in [57], is

$$\theta(\tau) = \arctan \frac{(b_1 + b_2 - a_1 - a_2)x_1(\tau) + (a_1a_2 - b_1b_2)}{\sqrt{(b_1 - a_1)(a_2 - b_1)(b_1 - a_1)(b_2 - a_2)}} - \arctan \frac{(b_1 + b_2 - a_1 - a_2)x_1(0) + (a_1a_2 - b_1b_2)}{\sqrt{(b_1 - a_1)(a_2 - b_1)(b_1 - a_1)(b_2 - a_2)}}, \quad (5.6)$$

where $x_1(\tau) \in [a_1, b_1]$ and $z(\tau) = z(0) + 2\pi\tau$.

From the figure, it could be seen that when the intervals are closer to each other or when the widths of them are bigger, the maximum point of $\tan[\theta(\tau)]$ would become higher. This then means that more information would be pulled out from one interval into the other, which then leads to the bigger values for entanglement and complexity of purification, as the modular flow through the minimal entanglement wedge cross section would be higher. So EoP and CoP would be proportional to θ .

From figure 14, it could be seen that increasing the length of the intervals would increase the maximum of $\tan[\theta(\tau)]$, but it does not change the minimum much. However, one could note that, still bigger intervals would have slightly bigger minimums.

Next, note that the operator reconstruction in entanglement wedge using mod-

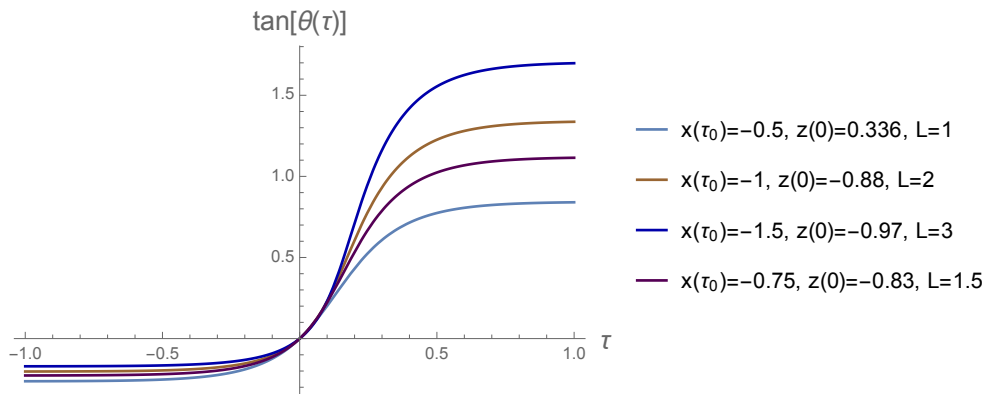


Figure 14. The plot of $\tan[\theta(\tau)]$ of [57] for various lengths of strips where the flow left mode and is passing exactly at the midpoint of the strip.

ular evolved boundary operators would be written as

$$\tilde{\Psi}_1(z(0)) = \frac{1}{\sin \theta(\tau)} e^{-i\mathbf{K}\tau} \tilde{\Psi}_2(z(\tau)) e^{i\mathbf{K}\tau} - \frac{1}{\tan \theta(\tau)} \tilde{\Psi}_2(z(0)) + \mathcal{O}(1/c). \quad (5.7)$$

The structure of this relation is again, two maps which used the modular flow and modular hamiltonian, and a projection. This combination is also what we have seen for the bulk reconstruction from quantum recovery channels such as Petz map, and connes cocycle flows. These operations indeed bring the information out to reconstruct the bulk.

The main point is that, the bigger the angle θ , the easier these projections would be performed and therefore the easier the modular flow and the bulk reconstruction would be. For the Petz map, these projections would be done by σ_A . So if the angle between ω_B and σ_A be bigger, it would be easier to “see” the information inside the peninsulas and therefore the Petz map and recovery channel could be implemented easier. This makes EoP and CoP bigger as the result.

6 Dynamics of Correlation Exchanges

For studying the “dynamics” of correlations among mixed systems, various models such as shockwaves, void formation, numerical models of quenches, etc, could be used which here we explain some of them briefly and employ them to get various results in our setup.

One motivation to study the dynamics would be to get further information on how gauge connections and curvature in the bulk gravitations would be related. For instance, one could study the emergence of the dynamics of gauge fields, in various setups such as *quenches* with different speeds and compare with the dynamics and shockwaves in the bulk.

Using the connection between modular chaos and Riemann curvature, one could also understand better how information between mixed states would propagate through the quantum channels and the recovery ones.

For studying the dynamical setup of [6] and how the excitations of CFT states would affect the modular Hamiltonians in the future causal cone, the Berry connection and the associated Berry phase, one could study the change of complexity of purification during quench similar to [72].

Then, using the quench setup, it could be understood how Berry connection could actually be promoted to a dynamical object. One could also do a similar study for the QCD case and check how confinement could change the holonomy and modular Berry curvature. Again, we expect that studying the EoP and CoP for this case, gives us further information on the relations between gauge connection and bulk curvature.

6.1 Information speed in mixed setup

First, we consider various measures for the speed of information and correlation exchanges among the mixed system. For example, our setup of moving these two strips closer to each other could be modeled by passing a shockwave. Then, using the results of [73], we could notice that the holonomy of the edge modes would measure the soft graviton component of the two shockwaves commutators.

Note that the spreading of information inside quantum channels is in “ballistic” form, with the speed of butterfly velocity “ v_B ”. The speed of spreading of the modular chaos would then be lower than v_B , since first these modes should create the bulk spacetimes and then the entanglement could spread inside it.

For tracking of the spreading of quantum information in mixed and pure states, we could also use properties of modular scrambling modes and its relation with the speed of information v_I , entanglement speed v_E , and the butterfly speed v_B . So one could try to depict a connection between these various speeds and the properties of the modular flow and modular Berry curvature.

Our setup of Figure 1, could also be modeled by considering the subsystem A as the input one where the information contained in it would expand ballistically toward the subsystem B , via the quantum channels, and bounce back via the recovery channels. These spreads of modular scrambling modes would be with the speed of $v_B = \sqrt{\frac{d}{2(d-1)}}$, and entanglement and mutual information would spread with the speed of $v_E = \frac{\sqrt{d(d-2)}^{\frac{1}{2}-\frac{1}{d}}}{[2(d-1)]^{1-\frac{1}{d}}}$. We actually expect that the information and modular chaos modes scramble with velocity v_B , but the minimum entanglement wedge and the cross section Γ would be created with velocity v_E , as it is related to the network depth and “vertical” direction of the channel. Note that in most cases we have $v_E \leq v_B$.

Also, the signature of the information speed of the dynamics of bulk curvature could be detected on the boundary CFT.

Similar to the studies of [72], the change of complexity and complexity of purification during a thermal quench could then be considered, which could give intuitions on the speed of correlation exchanges between mixed systems. In [72], entanglement of purification in the background of Vaidya-AdS spacetime has been worked out, where the metric is

$$ds^2 = \frac{1}{z^2} \left[-f(v, z)dv^2 - 2dzdv + dx^2 + \sum_{i=1}^{d-2} dy_i^2 \right],$$

$$f(v, z) = 1 - m(v)z^d. \quad (6.1)$$

The AdS radius is set to one and then the mass function could be taken as follows,

$$m(v) = \frac{M}{2} \left(1 + \tanh \frac{v}{v_0} \right), \quad (6.2)$$

where v_0 determines the quench speed.

In [72], for this background, the authors found that during the thermal quench, the critical separation D_c would initially increase with time and then decreases to a smaller value in the late times. They have also found that the holographic mutual information at first grows by time but then decreases to a smaller value than the initial one. These process could actually be explained by void formations which we will explain in the next subsection. Initially, voids would be created when the system could exchange information but then they would get absorbed. These process could also be explained using zero modes and modular flow. So first the flow of modular zero modes increases and it would reach to a maximum, and then when most of the mutual information have been exchanged, it would decrease. As has been found in [72], the equilibrium time would be approximately $l + D/2$, which is actually the time needed that the HRT surface of $2l + D$, and so $S_{2l+D}(t)$, reach equilibrium. At this time the voids have maximum size.

During the thermal quench, one could also track the changes in the *holonomy*, the change of the modular flow and as the result the change in the Berry curvature of the bulk, which in this case, could be similar to the passing of a shockwave in the geometry of the bulk, making the curvature increases at first and then it would decrease.

By considering the process using the behavior of quasiparticles, one could go into more details to check how information would become scrambled between the two intervals. In [74], the behavior of quantum information scrambling after a quantum quench has been studied. It was shown there, that the behavior of the decay would be different for integrable versus non-integrable systems, as for the later case, the decay

would be much faster and it was explained using the behavior of quasiparticles. This then would lead to the point that void formations and the stability of voids would be higher in integrable systems compared to the non-integrable ones. As the quasiparticles are non-stable or have short lifetime, voids would get absorbed faster as well.

The general point here is to understand how information from the initial state would spread throughout the system. For doing that one could study different quench scenarios in various setups. One important aspect of the dispersion of quantum information is that entanglement and correlations would disperse *globally* and in a non-local way, the fact that we have used in our new definition of *volume interval* in [9] as a definition of complexity of purification for mixed states.

In [74], it was proposed that in integrable systems, the “quasiparticles” would move ballistically and this way they would spread the initial correlations. This is also what we have observed by using the bit thread picture. However, note that after some time, this initial correlation would get dressed by the “many-body effect” and the thermodynamics of the system.

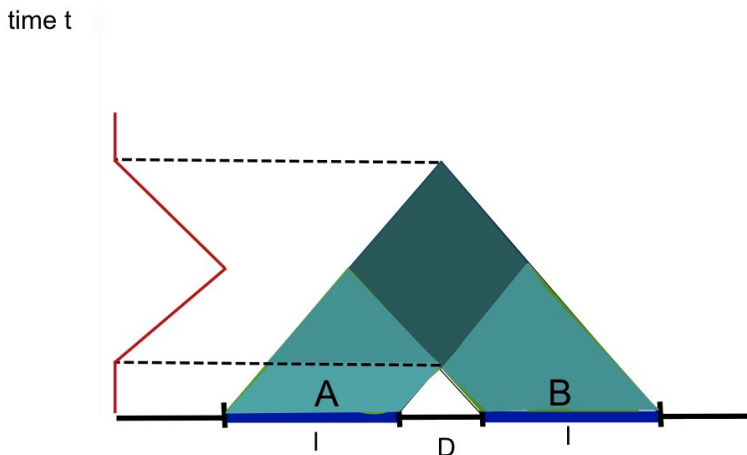


Figure 15. The mutual information behavior for two separated strips, $I_{A:B}$, in an integrable model, has been shown in the red line [74]. Note that at each time t , $I_{A:B}$ would be proportional to the width of darker region.

After a quantum quench, in integrable systems, the late time behavior of quasiparticles could be described by the “emergent thermodynamic macrostate or *Generalized Gibbs Ensemble (GGE)*” while for the non-integrable systems, it would be a thermal ensemble and the entanglement entropy of EPR pairs become the “thermodynamic” entropy of the stationary ensemble. Generally, then the non-integrable systems are better scramblers as there are no stable quasi-particles.

The connection between quasiparticles and mutual information could then be studied. In fact, there are infinite species of quasi-particles in integrable models where in [74] they were labelled by an integer n and the quasiparticles of the same species

were identified by the parameter “rapidity” λ , which for non-interacting particles would just be the momentum.

Usually in various condensed matter systems, where there are many degeneracies, bound Majorana fermions as the quasiparticle excitations, could appear which instead of acting as a single particle, would actually behave collectively with a “monoidal” or non-abelian statistics [75]. These non-abelian anyons have in fact practical applications in building topological quantum computers using fractional quantum Hall effect.

Note that, in figure 15, in our setup, we considered the case where each qubit at position x_i has a frequency ω_i and therefore has a localized lump of energy $E_i = \hbar\omega_i$. The solutions with $\omega = 0$, i.e, the zero modes, would lie on the corresponding HRRT surface which is along the thread connecting it to its pair. To go from one bit thread to another one, needs additional energy $\Delta E = \hbar\Delta\omega$ and therefore one needs to consider all the normal modes. These additional energy then create the curvature gradient in the bulk along the surface Γ . Note that the gradient of the flow of the modular zero modes would also be related to MERA and the tensor network structure.

If the qubits have additional charge or mass, ΔE would be different and therefore the bulk curvature and its gradient along Γ would change and as the result, EoP and CoP would also change.

For a single quasiparticle with fixed velocity $v(\lambda) = v$, the mutual information is

$$I_{A_1:A_2} = \max\left(\frac{d}{2}, vt\right) + \max\left(\frac{d+2\ell}{2}, vt\right) - 2\max\left(\frac{d+\ell}{2}, vt\right), \quad (6.3)$$

which is non-zero only for $d/(2v) < t < (d+2\ell)/(2v)$. Its maximum is at $t = (d+\ell)/(2v)$ and its height is proportional to ℓ which is the same result coming from holography.

For the general case of quasiparticles with non-trivial dispersion, the contribution of all the species of quasiparticles could be derived as

$$I_{A_1:A_2} = \sum_n I^{(n)} = \sum_n \int d\lambda s_n(\lambda) \left[\max\left(\frac{d}{2}, v_n(\lambda)t\right) + \max\left(\frac{d+2\ell}{2}, v_n(\lambda)t\right) - 2\max\left(\frac{d+\ell}{2}, v_n(\lambda)t\right) \right]. \quad (6.4)$$

It has been found that for the integrable models, the scrambling would follow an exponential behavior and the non-integrable cases would follow an algebraic behavior. One would expect that systems which have long-lived, but unstable quasiparticles such as confining models, have a cross over behavior between algebraic and exponential decay which could also be noticed from the behavior of modular Hamiltonian and void formations in QCD models.

Going back to the studied of speeds, in [76], the speed that quantum information would spread in chaotic systems has been discussed. The three speeds were,

information speed v_I , entanglement speed v_E which is related to the growth rate of entanglement after a quantum quench, and third the butterfly speed v_B which is related to the growth rate of perturbations spread in space. In [76], it has been shown that the relationship between these speeds would follow the relation

$$v_I = \frac{v_E(\epsilon, f)}{1 - f}. \quad (6.5)$$

Here, ϵ is the energy density of the initial state and f is the entanglement fraction. Note that the entanglement speed v_I has a range between $v_E(f = 0)$ to $v_B(f = 1)$.

The range for the speed of modular chaos could then be found. A speed for modular chaos could also be defined and its relationship with such speeds could be investigated. In fact, in [22], a bound for the speed of spread of modular scrambling modes has been found. As mentioned previously, after a perturbation, in the limit of $s \rightarrow \pm\infty$, the matrix elements of the modular Hamiltonian of a QFT subregion could not grow faster than $e^{2\pi s}$. For holographic CFTs, during the modular time of $1 \ll 2\pi s \ll \log N$, the growth of code subspace matrix elements of $\delta H_{\text{mod}}(s)$ has the bound [22]

$$\lim_{\substack{1 \ll N \\ 1 \ll 2\pi |s| \ll \log N}} \left| \frac{d}{ds} \log F_{ij}(s) \right| \leq 2\pi, \quad F_{ij}(s) = \left| \langle \chi_i | e^{iH_{\text{mod}}s} \delta H_{\text{mod}} e^{-iH_{\text{mod}}s} | \chi_j \rangle \right|.$$

There is a connection between this bound of 2π on the maximum rate of growth of modular scrambling modes, and entanglement and information speed which were mentioned before. Using that, the connections between Hayden-Preskill [77] protocol which tracks information as a function of time, and modular scrambling modes in modular time could be studied.

Finally note that, exactly at the critical distance between the intervals, and in the phase transition moment, the modular change, and the formation of the new structure for the modular flow would happen by the “tsunami velocity” which is bounded by the speed of light. Also as found in [78], the spread of the entanglement and also the modular flow would be highly sensitive to the initial entanglement pattern.

6.2 Void formation in mixed states

In [79], the void formation in CFTs and its links to black hole entropy and entanglement have been studied.

These void formations would have interesting implications for the multipartite structure of entanglement entropy and mutual information. In chaotic systems the distribution of voids would be random, but in our mixed states, the structure of such voids would be integrable, or even just plain “linear”. Therefore, further analysis of this void distribution in mixed states and the connection with EoP and CoP of entanglement wedge would be interesting.

As during the evolution of the system, the void formation is responsible for generating mutual information and multipartite entanglement among the disjoint intervals, we expect that entanglement and complexity of purification would be directly related to the probability of void formation as well. So the bigger the voids, the higher the mutual information between separated regions and also the higher the entanglement and complexity of purification. Also, the volume of the voids, and complexity and CoP, would be interconnected as well. On the other side, void formation could also be characterized and quantified by the number of quantum gates needed to purify the systems and therefore by the EoP and CoP.

Also, since for the same-sign charged and also dissipative systems, we would expect that the probability of void formations would be lower, then again we would arrive to the results we already got, that these parameters would decrease EoP and CoP as we have observed in [9] and also from other models studied here.

The probability of void formation for any operator O to form a void in any subsystem A or B is related to the correlations as

$$P_O^{(A)\text{or}(B)}(t) = \frac{\text{Tr}[(O^{(1)}(t))^\dagger O^{(1)}(t)]}{\text{Tr}(O^\dagger(t)O(t))}, \quad (6.6)$$

where the time-evolved operator $\mathcal{O}(t)$ could be written as

$$\mathcal{O}(t) = \mathcal{O}_1(t) + \mathcal{O}_2(t), \quad \mathcal{O}_1(t) = \tilde{\mathcal{O}}_{\bar{A}} \otimes \mathbf{1}_A. \quad (6.7)$$

An observation would be that the probability of evolution of an operator \mathcal{O}_α to another operator \mathcal{O}_β and also the capacity of quantum error correction channels are actually related. Under the time evolution we have

$$\mathcal{O}_\alpha(t) = U^\dagger(t)\mathcal{O}_\alpha U(t) = \sum_{\beta} c_\alpha^\beta(t)\mathcal{O}_\beta, \quad (6.8)$$

and $|c_\alpha^\beta(t)|^2$ is the probability of this evolution, which we conjecture is directly related to the channel capacity defined in 4.3 implying the connections between void formation and quantum error correction.

This number would also be related to the complexity and complexity of purification. More precisely

$$N_A(t) \equiv \sum_{\alpha \in I} \sum_{\beta \in A} |c_\alpha^\beta(t)|^2, \quad (6.9)$$

introduced in equation 2.11 of [79], which is the expected number of operators in the set I contained in A after passing the time t , would be connected to the complexity of state with density matrix $\rho_A(t)$. Also, the number

$$N(A, B; t) \equiv \sum_{\alpha \in I \cap B} \sum_{\beta \in A} |c_\alpha^\beta(t)|^2, \quad (6.10)$$

characterizes the number of initial operators in I from the region B which at time t would become contained in A . This number then would be related to the complexity of purification between regions A and B .

Another point worth to mention here is related to the linear growth of entanglement and complexity due to the “ballistic” operator growth, which would be true in both chaotic and integrable systems. This ballistic behavior of operators is also responsible for the decreasing behavior of EoP and CoP after decreasing the same sign-charges q and the dissipative parameter m .

Similarly, for other correlation measures, the number $\sum_{\alpha \in I \cap B} P_{O_\alpha^{(A)}}(t)$ could be used.

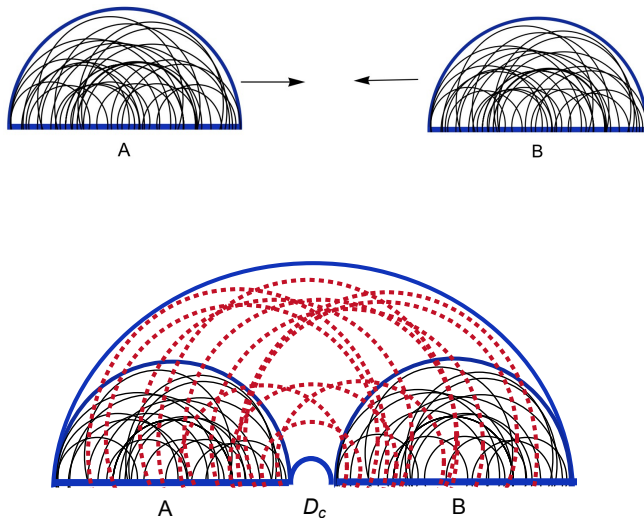


Figure 16. The creation of correlations at D_C is shown. This structures could also be explained using the void formation of [79].

We can then simulate our setup of two strips and the correlation evolution among them using the model of void creation. We could imagine that at first, i.e, $t = 0$, when the two subregions are far away from each other, the density operator for each one could be written as

$$\begin{aligned} \rho_{0A} &= |\psi\rangle \langle \psi| = \frac{1}{d} \mathbf{1} + \hat{\rho}_{0A}, & \text{Tr} \hat{\rho}_{0A} &= 0, \\ \rho_{0B} &= |\psi\rangle \langle \psi| = \frac{1}{d} \mathbf{1} + \hat{\rho}_{0B}, & \text{Tr} \hat{\rho}_{0B} &= 0. \end{aligned} \quad (6.11)$$

Then, after they become close enough to each other, similar to [79], we could write

$$\hat{\rho}(t) = \mathbf{1}_A \otimes O_B + O_A \otimes \mathbf{1}_B + \tilde{O}_A \otimes \tilde{O}_B. \quad (6.12)$$

The first term corresponds to the void formation in A , and the second one corresponds to the void formation in the subsystem B . Then, similar to the case of void formation between black hole and its radiation in [80], we could write

$$\rho_A = \frac{1}{d_A} \mathbf{1}_A + d_B O_A, \quad \rho_B = \frac{1}{d_B} \mathbf{1}_B + d_A O_B. \quad (6.13)$$

The reduced density matrix in the system A is related to the void formation in its complement including the system B and vice versa. Then, the EoP and CoP and modular flow evolution could be modeled by the probability plus the higher moments of these void formations. For the EoP case, the probability of void formation between A and A' to find $\rho_{AA'}$ and also between A and B to determine ρ_{AB} should be calculated. The first one would be proportional to $\frac{1}{d_B^2}$ and the second one would be proportional to $\frac{1}{d_A d_B}$, where d here denotes the dimension of the Hilbert space.

Similar to the story of the Page curve, the phase transitions between the two cases for the RT extremal surfaces and sudden appearance of the E_W case in the lower picture, could be related to the change of dominance between the identity and the void formation parts, as shown in figure 16. So considering

$$e^{-(n-1)S_n^{(A+B)}} = \frac{1}{d_A^{n-1}} + \frac{1}{d_B^{n-1}} + \dots + d_A^n \text{Tr}_B O_B^n + d_B^n \text{Tr}_A O_A^n, \quad (6.14)$$

the first two terms would be dominant before the phase transition and they are actually very small and close to zero, and the last two terms would dominate after the phase transition when the mutual information and EoP become non-zero as the two intervals get closer to each other to form mixed correlations. So different parts of the reduced density matrix in these series would become dominant at each stage. As one would expect, this behavior of correlation in the mixed setup would also be similar to behavior of replica wormholes in JT gravity studied recently in [14].

The modular operators mixing and correlation exchange and also the jump in mutual information between the two strips at the phase transition point, would be due to the transferring of information from the first strip to the second one, as shown in figure 16, then one could explain these and track information using the Hayden-Preskill like process. The second situation, could actually be considered as a typical state similar to BH case, and the results could be derived by averaging over the Hilbert space of the subsystems.

We expect that if the two subregions become close to each other fast enough, some aspects of modular chaos would behave in a way that we could dub them “modular vortices” where such new mathematical structures could be formulated using vortex dynamics. Also, the butterfly effects in modular chaos and modular scrambling modes could be noted there too. For any numerical simulation of the dynamics of exchange of correlations, operators and information between these states, for simplicity and for the first approximation, one could actually model these states

using the quantum Markov chains [81] where their pattern of correlation is very orderly. We leave the detailed numerical calculations for the future projects.

7 Discussion

In this work, various models of bulk reconstruction and the connections between them have been studied, specifically entanglement wedge reconstruction through modular Hamiltonian and modular flows and also quantum recovery channels, for a setup of mixed states of two intervals, have been investigated. Also, their connections with the behavior of mutual information, entanglement and complexity of purifications have been explored. Specifically, we used the results for EoP and CoP of a charged and massive gravity backgrounds and compared all the results with each other. The structures of zero modes and modular flows through minimal wedge cross section, explicitly for cases with dissipations and same sign charges have been probed.

The interconnections between quantum recovery channels, in particular the Petz map, and modular flow have been looked into where ideas such as eigenstate thermalization hypothesis have been used.

Furthermore, the links between modular Berry phase and complexity were probed further, where the already known behaviors of EoP and CoP have been used along the way. Also, the modular Hamiltonians for the connected versus disconnected entanglement wedge have been compared, specially the effects of singularities have been noticed. In addition, the effects of dissipations and charge on CC flows and kink transforms have been studied. Then, models of OPE block and specially the geodesic operator/OPE block dictionary for the bulk reconstruction have been looked over.

The “CFT Uhlmann phase/bulk symplectic form” dictionary also has been used to study the mixed entanglement wedge constructions and also the effects of dissipations and charge on each side have been discussed. We also commented on the connections with quantum capacity and modular Hamiltonian in this setup.

Next, to get better intuitions of the quantum correlations of mixed states in our setup, we studied a particular correlation measure and studied the effects of parameters such as mixing and mean photon numbers.

We also studied some exact forms of modular Hamiltonian in simple models and numerically investigated the effects of parameters such as lengths of strips and the distance between them.

We also commented on various information speeds in our mixed setup and the relationships among them and also with the bound on modular scrambling modes. In the study of the dynamical behaviors of correlations, we also considered void formations in our setup and the role they play in the phase transitions.

There are still many gaps in our studies that needed to be filled and points which should be studied in more precisions. For instance, many of the results could

be studied further numerically which we will get back to in the future works. Also, from the Tomita-Takesaki theory which studies modular flow in algebraic QFT, one could derive further constraints among the correlation functions which also could be useful in our setup of mixed states here.

Our studies was specifically for CFTs. These studies could also be done for Warped CFTs as well. So, for instance the holonomy of Berry connection along the path in the $U(1) \times SL(2, R)$ group manifold and the Berry phase on Virasoro-Kac-Moody orbits [82] could be studied. In [82], actually using the Maurer-Cartan form of the Virasoro group, the Berry phase had been computed. Using these calculations, the same could be done for the case of Kac-Moody as well and compare with the results we found for complexity in WCFTs [41, 43].

We could also check the logarithmic behavior of the complexity as noted in [35] for the case of warped AdS warped CFTs using the symmetry gates of this algebra, [41, 43, 83]. The connection with the path integral optimization proposal could also further be studied for this case, where the first steps have been taken in [41].

Also, recent ideas of the relationships between connecting CFTs and the dual domain walls in the AdS [84, 85], in our setup of entanglement wedge reconstruction, right in the moment when the two boundary regions become close enough, could be studied. One could imagine that the two regions are separated by some type of codimension-one brane and when the two regions become close enough, then the two corresponding branes collapse and merge with each other as shown in [84]. Similar to [84], the bulk region dual for each CFT could also have bulk matter and at the interface, one could consider a Gibbons-Hawking-York boundary term and another action for the matter on the brane. However, in [84] the tension of the interface brane is constant. However, one should note that based on our analysis in [9], this could not be true and the tension should in fact have a profile with a decreasing gradient.

These modular flows could also have some similarities with the “*fracton*” quantum matter states. The implications of Majorana islands could also be investigated for the case of modular flows in the mixed setups as well. For instance, if we imagine that we have a constant flow of energy into the mixed system which brings these two subsystems closer to each other with a constant speed, in spite of the existence of a force due to the entanglement, then the movement of the fractons and the connection with the mathematics of modular flows and modular chaos would be important and should be further studied. Specially for the case of massive gravity, the interactions between the fractons and gravitons would be very interesting, see [86, 87]. The connections between these models and the quantum universal recovery channels and modular Berry flows and also the bit-thread models could also be investigated.

Defining a notion of entanglement “monodromy”, specially for studying the structure of entanglement around singularities, similar to the notion of entanglement “holonomy” of [7], would also be interesting.

The connection between emergence of space, modular Berry flow and other novel

and interesting ideas such as AdS/Deep Learning or AdS/CFT as a deep Boltzmann machine [88] could be studied.

There should also be a connection between the applicability of replica trick and the specific properties of modular Hamiltonian which lead to the entanglement wedge reconstruction and the validity of Hayden-Preskill decoding criterion [13, 89]. The existence of multiple replicas, the ability of modular Hamiltonian to sews field theories, and the connectivity of geometries could be connected in more details. The Markovian properties of Hawking radiation and the modular Hamiltonian for the vacuum would actually support our guess. The symplectic form for the correlation between multipartite systems or between wormholes could also be studied.

The connections between all these arguments and the bulk reconstruction using the arguments of Hartle-Hawking wavefunction [90] would be compelling. The Wheeler-DeWitt wave function and its formalism could also be another method of bulk reconstruction. The Wheeler-DeWitt equation on each RT surface in the entanglement wedge cross section could be written as

$$\left(-\frac{1}{2}h^{-1/2}(h_{ik}h_{jl} + h_{il}h_{jk} - h_{ij}h_{kl})\frac{\delta^2}{\delta h_{ij}\delta h_{kl}} - R(h)h^{1/2} + 2\Lambda h^{1/2} \right)\Psi(h) = 0, \quad (7.1)$$

where R is the intrinsic curvature of any slice. For the mixed states we could also get a particular differential equation for the small variation of h as $|h + \delta h\rangle$. Connecting this relation to gravitational on-shell action and then to the Uhlmann phase, then could give a new formulation for complexity as well.

In the picture of traversable wormhole of [91], the coupling in the form of $V = \frac{g}{n} \sum_{i=1}^n Z_i^L Z_i^R$ has been added where g is small and n is large which in the bulk has the net effect of pushing the signal down and make the teleporting between the two boundaries possible. The effects of such terms in our structure, for transformation of information between the two subsystems and the net effects on the phase transitions could then studied.

Very recently, in [92], a new formula for the massive modular Hamiltonian of a unit space ball at a origin B , has been found as

$$K_B^m = \begin{bmatrix} 0 & M \\ L_m & 0 \end{bmatrix}, \quad (7.2)$$

where

$$L_m = \frac{1}{2}(1 - r^2)(\nabla^2 - m^2) - r\partial_r - D - \frac{1}{2}m^2 G_m^B, \quad (7.3)$$

where also G_m^B is the Green's function associated to the operator $H_m = -\nabla^2 + m^2$ which for $d = 3$ is

$$G_m^B f(x) = \frac{1}{4\pi} \int_B \frac{e^{-m|x-y|}}{|x-y|} f(y) dy. \quad (7.4)$$

As it could be seen, the mass parameter m decreases the matrix element of modular Hamiltonian L_m . It would be interesting to exactly check how m also affects various mixed correlations, CC modular flow, scrambling modes, quantum recovery channels, etc, using this formula. Also, note that the Green's function has a form of Yukawa potential $e^{-mr}/4\pi r$ which could be used for removing the singularity of phase diagrams of mutual information.

These methods of entanglement wedge reconstruction and emergence of bulk spacetimes could also be connected to the new studies of mechanism of precision microstates counting of black hole entropy using topologically twisted index [93], localization techniques, Bethe-ansatz formulation and \mathcal{I} -extremization. This point came to mind because of the procedure they employed as they uses imaginary chemical potentials to find the number of black hole microstates which then would lead to the imaginary result for the complexity of purification of mixed states as we found. We hope to address some of these problems in the future works.

Acknowledgement

I would like to thank Mahdi Torabian and Xiaomei Kuang for their help and supports and for useful discussions. This work has been supported by Iran's National Elites Foundation (INEF) and Chinese Postdoctoral Science Foundation.

References

- [1] A. Hamilton, D. N. Kabat, G. Lifschytz, and D. A. Lowe, *Holographic representation of local bulk operators*, *Phys. Rev.* **D74** (2006) 066009, [[hep-th/0606141](#)].
- [2] X. Dong, D. Harlow, and A. C. Wall, *Reconstruction of Bulk Operators within the Entanglement Wedge in Gauge-Gravity Duality*, *Phys. Rev. Lett.* **117** (2016), no. 2 021601, [[arXiv:1601.05416](#)].
- [3] A. Almheiri, X. Dong, and D. Harlow, *Bulk Locality and Quantum Error Correction in AdS/CFT*, *JHEP* **04** (2015) 163, [[arXiv:1411.7041](#)].
- [4] T. Faulkner and A. Lewkowycz, *Bulk locality from modular flow*, *JHEP* **07** (2017) 151, [[arXiv:1704.05464](#)].
- [5] N. Bao, C. Cao, S. Fischetti, and C. Keeler, *Towards Bulk Metric Reconstruction from Extremal Area Variations*, *Class. Quant. Grav.* **36** (2019), no. 18 185002, [[arXiv:1904.04834](#)].
- [6] B. Czech, J. de Boer, D. Ge, and L. Lamprou, *A Modular Sewing Kit for Entanglement Wedges*, [[arXiv:1903.04493](#)].
- [7] B. Czech, L. Lamprou, and L. Susskind, *Entanglement Holonomies*, [[arXiv:1807.04276](#)].

- [8] B. Czech, L. Lamprou, S. Mccandlish, and J. Sully, *Modular Berry Connection for Entangled Subregions in AdS/CFT*, *Phys. Rev. Lett.* **120** (2018), no. 9 091601, [[arXiv:1712.07123](#)].
- [9] M. Ghodrati, X.-M. Kuang, B. Wang, C.-Y. Zhang, and Y.-T. Zhou, *The connection between holographic entanglement and complexity of purification*, *JHEP* **09** (2019) 009, [[arXiv:1902.02475](#)].
- [10] J. Cotler, P. Hayden, G. Penington, G. Salton, B. Swingle, and M. Walter, *Entanglement Wedge Reconstruction via Universal Recovery Channels*, *Phys. Rev.* **X9** (2019), no. 3 031011, [[arXiv:1704.05839](#)].
- [11] B. Czech, L. Lamprou, S. McCandlish, B. Mosk, and J. Sully, *A Stereoscopic Look into the Bulk*, *JHEP* **07** (2016) 129, [[arXiv:1604.03110](#)].
- [12] J. Kirklin, *The Holographic Dual of the Entanglement Wedge Symplectic Form*, *JHEP* **01** (2020) 071, [[arXiv:1910.00457](#)].
- [13] C.-F. Chen, G. Penington, and G. Salton, *Entanglement Wedge Reconstruction using the Petz Map*, [arXiv:1902.02844](#).
- [14] G. Penington, S. H. Shenker, D. Stanford, and Z. Yang, *Replica wormholes and the black hole interior*, [arXiv:1911.11977](#).
- [15] S. H. Hendi, B. Eslam Panah, and S. Panahiyan, *Massive charged BTZ black holes in asymptotically (a)dS spacetimes*, *JHEP* **05** (2016) 029, [[arXiv:1604.00370](#)].
- [16] M. Blake and D. Tong, *Universal Resistivity from Holographic Massive Gravity*, *Phys. Rev.* **D88** (2013), no. 10 106004, [[arXiv:1308.4970](#)].
- [17] T. Takayanagi and K. Umemoto, *Entanglement of purification through holographic duality*, *Nature Phys.* **14** (2018), no. 6 573–577, [[arXiv:1708.09393](#)].
- [18] D. L. Jafferis, A. Lewkowycz, J. Maldacena, and S. J. Suh, *Relative entropy equals bulk relative entropy*, *JHEP* **06** (2016) 004, [[arXiv:1512.06431](#)].
- [19] D. L. Jafferis and S. J. Suh, *The Gravity Duals of Modular Hamiltonians*, *JHEP* **09** (2016) 068, [[arXiv:1412.8465](#)].
- [20] H. Casini, E. Teste, and G. Torroba, *Modular Hamiltonians on the null plane and the Markov property of the vacuum state*, *J. Phys.* **A50** (2017), no. 36 364001, [[arXiv:1703.10656](#)].
- [21] G. Wong, *A note on entanglement edge modes in Chern Simons theory*, *JHEP* **08** (2018) 020, [[arXiv:1706.04666](#)].
- [22] J. De Boer and L. Lamprou, *Holographic Order from Modular Chaos*, *JHEP* **06** (2020) 024, [[arXiv:1912.02810](#)].
- [23] O. M. Pimentel, G. A. Gonzalez, and F. D. Lora.Clavijo, *The Energy Momentum Tensor for a Dissipative Fluid in General Relativity*, *Gen. Rel. Grav.* **48** (2016), no. 10 124, [[arXiv:1604.01318](#)].

- [24] M. Baggioli, M. Vasin, V. V. Brazhkin, and K. Trachenko, *Field Theory of Dissipative Systems with Gapped Momentum States*, [arXiv:2004.13613](#).
- [25] A. Gilyen, S. Lloyd, I. Marvian, Y. Quek, and M. M. Wilde, *Quantum algorithm for Petz recovery channels and pretty good measurements*, [arXiv:2006.16924](#).
- [26] D. Petz, *Sufficient subalgebras and the relative entropy of states of a von neumann algebra*, *Comm. Math. Phys.* **105** (1986), no. 1 123–131.
- [27] M. Junge, R. Renner, D. Sutter, M. M. Wilde, and A. Winter, *Universal recovery maps and approximate sufficiency of quantum relative entropy*, *Annales Henri Poincaré* **19** (2018), no. 10 2955–2978.
- [28] M. Alishahiha, *Holographic Complexity*, *Phys. Rev.* **D92** (2015), no. 12 126009, [[arXiv:1509.06614](#)].
- [29] F. G. S. L. Brandao, E. Crosson, M. B. “ahino’lu, and J. Bowen, *Quantum Error Correcting Codes in Eigenstates of Translation-Invariant Spin Chains*, *Phys. Rev. Lett.* **123** (2019), no. 11 110502, [[arXiv:1710.04631](#)].
- [30] V. V. A. G. S. F. P. P. H. P. Faist, S. Nezami and t. . J. Preskill.
- [31] H. Kwon and M. S. Kim, *Fluctuation theorems for a quantum channel*, *Phys. Rev. X* **9** (Aug, 2019) 031029.
- [32] V. Khemani, A. Vishwanath, and D. A. Huse, *Operator spreading and the emergence of dissipation in unitary dynamics with conservation laws*, *Phys. Rev.* **X8** (2018), no. 3 031057, [[arXiv:1710.09835](#)].
- [33] C. A. Agon, M. Headrick, and B. Swingle, *Subsystem Complexity and Holography*, *JHEP* **02** (2019) 145, [[arXiv:1804.01561](#)].
- [34] M. M. Wolf, F. Verstraete, M. B. Hastings, and J. I. Cirac, *Area Laws in Quantum Systems: Mutual Information and Correlations*, *Phys. Rev. Lett.* **100** (2008), no. 7 070502, [[arXiv:0704.3906](#)].
- [35] I. Akal, *Reflections on Virasoro circuit complexity and Berry phase*, [arXiv:1908.08514](#).
- [36] R. Resta, *Review article: Manifestations of berry’s phase in molecules and condensed matter*, 2000.
- [37] D. Xiao, M.-C. Chang, and Q. Niu, *Berry phase effects on electronic properties*, *Rev. Mod. Phys.* **82** (Jul, 2010) 1959–2007.
- [38] T. Faulkner, R. G. Leigh, O. Parrikar, and H. Wang, *Modular Hamiltonians for Deformed Half-Spaces and the Averaged Null Energy Condition*, *JHEP* **09** (2016) 038, [[arXiv:1605.08072](#)].
- [39] H. A. Camargo, M. P. Heller, R. Jefferson, and J. Knaute, *Path integral optimization as circuit complexity*, *Phys. Rev. Lett.* **123** (2019), no. 1 011601, [[arXiv:1904.02713](#)].
- [40] P. Caputa, N. Kundu, M. Miyaji, T. Takayanagi, and K. Watanabe, *Liouville Action*

- as Path-Integral Complexity: From Continuous Tensor Networks to AdS/CFT, *JHEP* **11** (2017) 097, [[arXiv:1706.07056](#)].
- [41] M. Ghodrati, *Complexity and emergence of warped AdS₃ space-time from chiral Liouville action*, *JHEP* **02** (2020) 052, [[arXiv:1911.03819](#)].
- [42] M. V. Berry, *Quantal phase factors accompanying adiabatic changes*, *Proceedings of the royal society A* (1984).
- [43] M. Ghodrati, *Complexity growth in massive gravity theories, the effects of chirality, and more*, *Phys. Rev.* **D96** (2017), no. 10 106020, [[arXiv:1708.07981](#)].
- [44] A. R. Brown, H. Gharibyan, A. Streicher, L. Susskind, L. Thorlacius, and Y. Zhao, *Falling Toward Charged Black Holes*, *Phys. Rev.* **D98** (2018), no. 12 126016, [[arXiv:1804.04156](#)].
- [45] M. Ghodrati, *Complexity growth rate during phase transitions*, *Phys. Rev.* **D98** (2018), no. 10 106011, [[arXiv:1808.08164](#)].
- [46] F. Pastawski, B. Yoshida, D. Harlow, and J. Preskill, *Holographic quantum error-correcting codes: Toy models for the bulk/boundary correspondence*, *JHEP* **06** (2015) 149, [[arXiv:1503.06237](#)].
- [47] S. R. Das, S. Hampton, and S. Liu, *Quantum Quench in Non-relativistic Fermionic Field Theory: Harmonic traps and 2d String Theory*, *JHEP* **08** (2019) 176, [[arXiv:1903.07682](#)].
- [48] F. Wilczek and A. Zee, *Appearance of Gauge Structure in Simple Dynamical Systems*, *Phys. Rev. Lett.* **52** (1984) 2111–2114.
- [49] M. Ghodrati, *Schwinger Effect and Entanglement Entropy in Confining Geometries*, *Phys. Rev.* **D92** (2015), no. 6 065015, [[arXiv:1506.08557](#)].
- [50] Y. Nakata, T. Takayanagi, Y. Taki, K. Tamaoka, and Z. Wei, *Holographic Pseudo Entropy*, [arXiv:2005.13801](#).
- [51] A. R. Brown, H. Gharibyan, S. Leichenauer, H. W. Lin, S. Nezami, G. Salton, L. Susskind, B. Swingle, and M. Walter, *Quantum Gravity in the Lab: Teleportation by Size and Traversable Wormholes*, [arXiv:1911.06314](#).
- [52] R. E. Arias, H. Casini, M. Huerta, and D. Pontello, *Entropy and modular Hamiltonian for a free chiral scalar in two intervals*, *Phys. Rev. D* **98** (2018), no. 12 125008, [[arXiv:1809.00026](#)].
- [53] S. Balakrishnan and O. Parrikar, *Modular Hamiltonians for Euclidean Path Integral States*, [arXiv:2002.00018](#).
- [54] N. Lashkari, H. Liu, and S. Rajagopal, *Modular Flow of Excited States*, [arXiv:1811.05052](#).
- [55] R. Bousso, V. Chandrasekaran, P. Rath, and A. Shahbazi-Moghaddam, *Gravity Dual of Connes Cocycle Flow*, [arXiv:2007.00230](#).

- [56] A. Levine, A. Shahbazi-Moghaddam, and R. M. Soni, *Seeing the Entanglement Wedge*, [arXiv:2009.11305](#).
- [57] Y. Chen, *Pulling Out the Island with Modular Flow*, *JHEP* **03** (2020) 033, [[arXiv:1912.02210](#)].
- [58] B. Chen, B. Czech, and Z.-z. Wang, *Cutoff Dependence and Complexity of the CFT_2 Ground State*, [arXiv:2004.11377](#).
- [59] B. Carneiro da Cunha and M. Guica, *Exploring the BTZ bulk with boundary conformal blocks*, [arXiv:1604.07383](#).
- [60] N. Engelhardt and G. T. Horowitz, *Recovering the spacetime metric from a holographic dual*, *Adv. Theor. Math. Phys.* **21** (2017) 1635–1653, [[arXiv:1612.00391](#)].
- [61] N. Engelhardt and G. T. Horowitz, *Towards a Reconstruction of General Bulk Metrics*, *Class. Quant. Grav.* **34** (2017), no. 1 015004, [[arXiv:1605.01070](#)].
- [62] A. May, G. Penington, and J. Sorce, *Holographic scattering requires a connected entanglement wedge*, [arXiv:1912.05649](#).
- [63] S. G. A. W. S. F. M. M.-D. O. Viyuela, A. Rivas, *Observation of topological Uhlmann phases with superconducting qubits*, *Nature* **01** (2016) 071, [[arXiv:1607.08778](#)].
- [64] J. Koch, T. M. Yu, J. Gambetta, A. A. Houck, D. I. Schuster, J. Majer, A. Blais, M. H. Devoret, S. M. Girvin, and R. J. Schoelkopf, *Charge-insensitive qubit design derived from the cooper pair box*, *Phys. Rev. A* **76** (Oct, 2007) 042319.
- [65] M. Ghodrati and D. Gregoris, *On the Curvature Invariants of the Massive Banados-Teitelboim-Zanelli Black Holes and Their Holographic Pictures*, [arXiv:2003.04412](#).
- [66] K. Papadodimas and S. Raju, *State-Dependent Bulk-Boundary Maps and Black Hole Complementarity*, *Phys. Rev.* **D89** (2014), no. 8 086010, [[arXiv:1310.6335](#)].
- [67] J. Q. X. Liu, L.; Hou, *Quantum Correlation Based on Uhlmann Fidelity for Gaussian States*, [Entropy](#) **2019**.
- [68] R. Abt and J. Erdmenger, *Properties of Modular Hamiltonians on Entanglement Plateaux*, *JHEP* **11** (2018) 002, [[arXiv:1809.03516](#)].
- [69] Y. Suzuki, T. Takayanagi, and K. Umemoto, *Entanglement Wedges from Information Metric in Conformal Field Theories*, [arXiv:1908.09939](#).
- [70] K. Ghoroku, K. Kashiwa, Y. Nakano, M. Tachibana, and F. Toyoda, *Extension to Imaginary Chemical Potential in a Holographic Model*, [arXiv:2005.14416](#).
- [71] H. Casini and M. Huerta, *Reduced density matrix and internal dynamics for multicomponent regions*, *Class. Quant. Grav.* **26** (2009) 185005, [[arXiv:0903.5284](#)].
- [72] R.-Q. Yang, C.-Y. Zhang, and W.-M. Li, *Holographic entanglement of purification for thermofield double states and thermal quench*, *JHEP* **01** (2019) 114, [[arXiv:1810.00420](#)].

- [73] J. Maldacena, S. H. Shenker, and D. Stanford, *A bound on chaos*, *JHEP* **08** (2016) 106, [[arXiv:1503.01409](#)].
- [74] V. Alba and P. Calabrese, *Quantum information scrambling after a quantum quench*, *Phys. Rev.* **B100** (2019), no. 11 115150, [[arXiv:1903.09176](#)].
- [75] A. Stern, *Non-Abelian states of matter*, *Nature* **120** (2010), no. 9 091601.
- [76] J. Couch, S. Eccles, P. Nguyen, B. Swingle, and S. Xu, *The Speed of Quantum Information Spreading in Chaotic Systems*, [arXiv:1908.06993](#).
- [77] P. Hayden and J. Preskill, *Black holes as mirrors: Quantum information in random subsystems*, *JHEP* **09** (2007) 120, [[arXiv:0708.4025](#)].
- [78] H. Casini, H. Liu, and M. Mezei, *Spread of entanglement and causality*, *JHEP* **07** (2016) 077, [[arXiv:1509.05044](#)].
- [79] H. Liu and S. Vardhan, *Void Formation in Operator Growth, Entanglement, and Unitarity*, [arXiv:1912.08918](#).
- [80] H. Liu and S. Vardhan, *A dynamical mechanism for the Page curve from quantum chaos*, [arXiv:2002.05734](#).
- [81] P. Hayden, R. Jozsa, D. Petz, and A. Winter, *Structure of states which satisfy strong subadditivity of quantum entropy with equality*, *Communications in Mathematical Physics* **246** (2004), no. 2 359–374.
- [82] B. Oblak, *Berry Phases on Virasoro Orbits*, *JHEP* **10** (2017) 114, [[arXiv:1703.06142](#)].
- [83] M. Ghodrati and A. Naseh, *Phase transitions in Bergshoeff-Hohm-Townsend massive gravity*, *Class. Quant. Grav.* **34** (2017), no. 7 075009, [[arXiv:1601.04403](#)].
- [84] P. Simidzija and M. Van Raamsdonk, *Holo-ween*, 2020. [arXiv:2006.13943](#).
- [85] H. Ooguri and T. Takayanagi, *Cobordism Conjecture in AdS*, [arXiv:2006.13953](#).
- [86] M. Pretko, *Emergent gravity of fractons: Mach’s principle revisited*, *Phys. Rev. D* **96** (Jul, 2017) 024051.
- [87] H. Yan, *Hyperbolic fracton model, subsystem symmetry, and holography*, *Phys. Rev. B* **99** (Apr, 2019) 155126.
- [88] K. Hashimoto, *AdS/CFT correspondence as a deep Boltzmann machine*, *Phys. Rev.* **D99** (2019), no. 10 106017, [[arXiv:1903.04951](#)].
- [89] G. Penington, *Entanglement Wedge Reconstruction and the Information Paradox*, [arXiv:1905.08255](#).
- [90] D. L. Jafferis, *Bulk reconstruction and the Hartle-Hawking wavefunction*, [arXiv:1703.01519](#).
- [91] P. Gao, D. L. Jafferis, and A. C. Wall, *Traversable Wormholes via a Double Trace Deformation*, *JHEP* **12** (2017) 151, [[arXiv:1608.05687](#)].
- [92] R. Longo and G. Morsella, *The massive modular Hamiltonian*, [arXiv:2012.00565](#).

- [93] F. Benini and A. Zaffaroni, *A topologically twisted index for three-dimensional supersymmetric theories*, *JHEP* **07** (2015) 127, [[arXiv:1504.03698](#)].